

# The Bacterial Cytoskeleton

Yu-Ling Shih† and Lawrence Rothfield\*

*Department of Molecular, Microbial and Structural Biology, University of Connecticut Health Center,  
 263 Farmington Avenue, Farmington, Connecticut 06032*

<b>INTRODUCTION .....</b>	<b>730</b>
<b>BACTERIAL CYTOSKELETAL ELEMENTS.....</b>	<b>730</b>
<b>Actin Homologs .....</b>	<b>730</b>
MreB and MreB homologs .....	730
(i) Cytoskeletal organization of MreB proteins.....	731
(ii) MreB polymerization and depolymerization .....	733
(iii) Cellular functions of MreB and MreB homologs.....	733
Plasmid partitioning by an actin homolog: the ParM system.....	736
(i) ParM polymer assembly and disassembly .....	736
(ii) Mechanism of ParM function .....	737
(iii) Filament disassembly and plasmid migration.....	737
MamK.....	738
<b>Tubulin Homologs .....</b>	<b>738</b>
FtsZ.....	738
(i) The FtsZ ring.....	738
(ii) Membrane attachment of the Z-ring.....	739
(iii) FtsZ spiral structures .....	739
(iv) FtsZ polymerization and depolymerization .....	740
(v) Regulation of Z-ring assembly and stability.....	740
BtubA/B .....	741
(i) BtubA/B polymerization .....	741
Microtubule-like structures in <i>Verrucomicrobia</i> .....	741
<b>Intermediate Filament Protein Homologs .....</b>	<b>741</b>
Crescentin .....	741
<b>The MinD/ParA Class of Bacterial Cytoskeletal Proteins .....</b>	<b>742</b>
<b>Subgroup 1: MinD .....</b>	<b>742</b>
(i) The MinCDE system.....	742
(ii) The MinD cytoskeleton.....	742
(iii) MinD structure.....	743
(iv) MinD polymerization .....	743
(v) Membrane targeting of MinD.....	744
(vi) MinD-bilayer interactions .....	744
(vii) Dynamic rearrangements of the MinD cytoskeleton.....	745
<b>Subgroup 2: type I plasmid partitioning proteins .....</b>	<b>745</b>
(i) ParA/B proteins in plasmid partitioning.....	746
(ii) ParA cytoskeletal structures .....	746
(iii) ParA polymerization .....	746
(iv) ParA oscillation .....	746
Soj .....	747
<b>Other Filamentous Intracellular Structures.....</b>	<b>748</b>
<i>Spiroplasma melliferum</i> fibrillar structures .....	748
<i>Treponema phagodenis</i> cytoplasmic filaments .....	748
<i>Myxococcus xanthus</i> intracellular filaments .....	748
<i>Mycoplasma pneumoniae</i> filamentous structures .....	748
Miscellaneous intracellular structures .....	748
<b>HELICES, HELICES, AND MORE HELICES.....</b>	<b>748</b>
SetB.....	748
Sec Proteins .....	749
Tar.....	749

\* Corresponding author. Mailing address: Department of Molecular, Microbial and Structural Biology, University of Connecticut Health Center, 263 Farmington Avenue, Farmington, CT 06032. Phone: (860) 679-3581. Fax: (860) 6789-1239. E-mail: lroth@neuron.uchc.edu.

† Present address: Institute of Biological Chemistry, Academia Sinica, 128 Sec. 2, Academia Rd., Nankang, Taipei 115, Taiwan.

Outer Membrane Components .....	749
Why Is the Helical Distribution Pattern So Popular? .....	749
EUKARYOTIC AND PROKARYOTIC CYTOSKELETAL ELEMENTS .....	749
Properties and Functional Relationships.....	749
Membrane-Associated Cytoskeletal Structures .....	750
CONCLUSIONS AND SUMMARY.....	750
ACKNOWLEDGMENTS .....	750
REFERENCES .....	750

## INTRODUCTION

It is truly breathtaking that within a period of 5 years a longstanding "truth" about one of the major life forms of the planet has been overturned. Although there had been previous indications of organized structures within bacterial cells (18, 139, 209), including the demonstration by Bi and Lutkenhaus that the tubulin homolog FtsZ forms a ring-like structure at the division site (15), the period of rapid advance began with the discovery by Jones et al. in 2001 that bacterial actin homologs in *Bacillus subtilis* are organized into extended helical structures that play key roles in cell shape regulation (95). Since then, the dictum that bacteria have no long-range internal structure has been replaced by the realization that the interior of the bacterial cell contains a large number of organized cytoskeletal elements, probably with a much larger group of cytoskeleton-associated components still to be discovered. Especially impressive is the large amount of information that has been revealed during this relatively short time span. It is now known that bacterial cytoskeletal homologs exist for all of the main groups of eukaryotic cytoskeletal proteins, i.e., the actin, tubulin, and intermediate filament (IF) groups. However, important differences between the eukaryotic and prokaryotic cytoskeletal systems have also emerged. These include the discovery that there is at least one major group of bacterial cytoskeletal elements, the MinD/ParA group, that has no known eukaryotic counterpart and the finding that analogous functions are frequently carried out by different cytoskeletal classes in eukaryotes and prokaryotes, often using different mechanisms.

The definition of the eukaryotic cytoskeleton has evolved over the past half century. It includes both stable filamentous structures that are composed largely of intermediate filament proteins and dynamic structures such as tubulin-derived microtubular structures and actin filaments that can assemble, disassemble, and redistribute rapidly within the cell in response to signals that regulate cellular functions such as cell cycle progression, intracellular organelle transport, motility, and cell shape. The common characteristics of these systems are their polymeric filamentous nature and their long-range order within the cell. Based on this background, we define bacterial cytoskeletal structures as filamentous structures that are based primarily on polymers of a single class of protein, that show long-range order within the cell, and, where this has been studied, that are capable of self-assembling in vitro into extended polymeric filaments. The bacterial cytoskeleton consists of the several groups of intracellular structures that meet this definition.

In this review we attempt to synthesize the wide range of information that is now available about the bacterial cytoskeleton, concentrating on systems where sufficient information is

available to draw significant conclusions. We emphasize the cytoskeletal aspects of these systems and the relation of their cytoskeletal organization to specific cellular functions. We deal relatively briefly with some details of biological function that have recently been reviewed elsewhere or that may not involve the cytoskeleton. Where applicable, we refer the reader to recent reviews on these topics.

## BACTERIAL CYTOSKELETAL ELEMENTS

### Actin Homologs

Several actin homologs that form cytoskeletal structures are present in bacterial cells. The three bacterial actin homologs whose three-dimensional structures are known show significant structural similarity to eukaryotic actin (Fig. 1A) (171, 214, 216) despite a variable degree of sequence similarity. They share a similar actin fold, which is characteristic of the actin superfamily, with the most conserved region being the actin ATPase domain (16). Other bacterial proteins of the actin superfamily that are not known to be cytoskeletal elements also exist. These include, for example, cell division protein FtsA (discussed below), the protein chaperone DnaK (Hsp70), and sugar hexokinases (16).

In eukaryotic cells, actin polymerizes into polarized structures, with addition of actin-ATP being favored at one end and ATP hydrolysis and subunit release being favored at the other. This can result in rapid displacement of the filament, due to extension at one end and shrinkage at the other, or in rapid changes in filament size, number, or topological distribution in response to regulatory inputs. Actin filaments are usually associated with a number of other proteins that play regulatory roles in the dynamics of filament growth, disassembly, cleavage, bundling, etc. (reviewed in references 4 and 164). Similar filament-associated regulatory elements have not yet been identified for most bacterial actin homologs.

We discuss here the best-studied bacterial actin-like cytoskeletal proteins, i.e., MreB, ParM, and MamK.

**MreB and MreB homologs.** MreB and MreB homologs are actin-related cytoskeletal proteins that play an important role in a number of cellular functions in bacteria, including regulation of cell shape, chromosome segregation, cell polarity, and organization of membranous organelles. Some bacterial species, such as *Escherichia coli*, contain a single MreB protein. Others contain two or more MreB-related proteins, such as the *Bacillus subtilis* MreB, Mbl (MreB-like), and MreBH (MreB homolog) proteins (1, 117, 217).

In many organisms, such as *E. coli* and *B. subtilis*, *mreB* is part of an operon that also contains genes coding for the MreC and MreD proteins. MreB, MreC, and MreD are required for cell viability (107, 113, 115). The loss of viability of *E. coli*

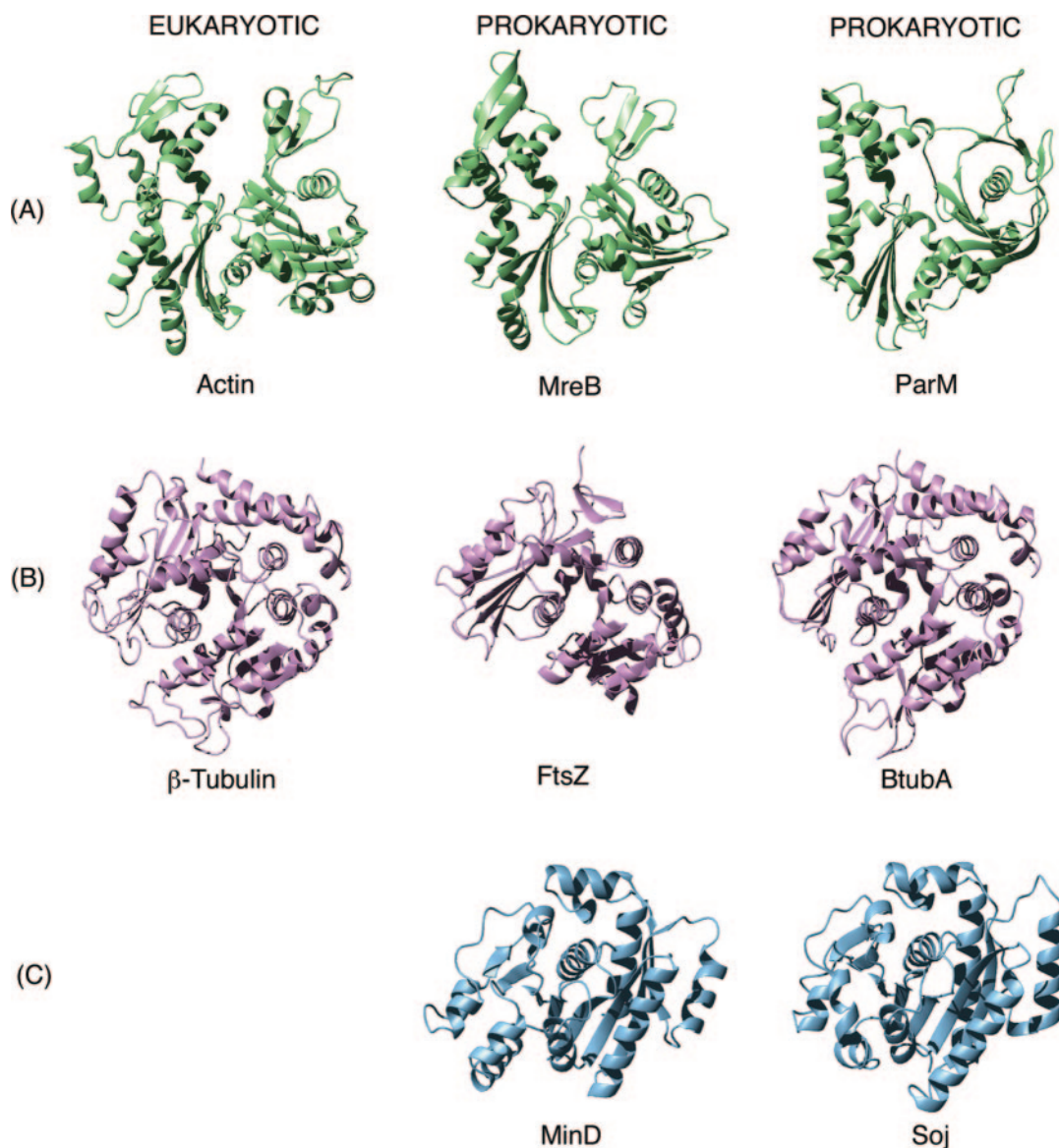


FIG. 1. Structural comparison of eukaryotic and prokaryotic cytoskeletal proteins. Protein structures were downloaded from the Protein Data Bank (PDB) (<http://www.rcsb.org/pdb/>) and aligned using the EMBL-EBI Dali server (<http://www.ebi.ac.uk/dali/>). Protein structures were then analyzed and displayed using the MolMol program (103). Nucleotides and inorganic molecules that cocrystallized with the proteins are not shown. (A) Actin homologs. From left to right: *Saccharomyces cerevisiae* actin (PDB entry 1YAGA), ATP bound (218); *Thermotoga maritima* MreB (PDB entry 1JCG), AMPPNP bound (214); ParM of plasmid R1 (PDB entry 1MWM), ADP bound (216). (B) Tubulin homologs. From left to right: *Bos taurus*  $\beta$ -tubulin (PDB entry 1JFFB), GTP/GDP bound (124); *Methanococcus jannaschii* FtsZ (PDB entry 1FSZ), GDP bound (122); *Prostheco-bacter dejongei* BtubA (PDB entry 2BTOA), GTP bound (183). (C) MinD (left) and Soj (right) proteins: *Archaeoglobus fulgidus* MinD (PDB entry 1HYQ), nucleotide free (24); *Thermus thermophilus* Soj (PDB entry 2BEJ), ADP bound (116). The topological specificity domain of the MinE dimer is shown (residues 31 to 88). The MinD-binding domains of each monomer extend from opposite sides (the right and left sides in this view) of the dimeric topological specificity domain (100).

$\Delta mreB$  cells can be suppressed by modest overexpression of the essential cell division gene FtsZ (107, 188). It was suggested that this reflects a need for more FtsZ because of the larger volume of the spherical MreB-depleted cells (107). It is possible that the viable *mreB* mutant strains that have been isolated contain elevated cellular FtsZ levels due to secondary suppressor mutations.

(i) **Cytoskeletal organization of MreB proteins.** The cellular organization of MreB and MreB homologs in *Escherichia coli*,

*Bacillus subtilis*, *Caulobacter crescentus*, and *Rhodobacter sphaeroides* has been described (53, 60, 95, 108, 187, 191). In all cases the proteins are organized into helical filamentous structures that coil around the rod-shaped cell, as shown by immunofluorescence microscopy and fluorescence microscopy of cells expressing fusions of the proteins to green fluorescent protein (GFP) or one of its derivatives, such as yellow fluorescent protein (YFP) (Fig. 2A and B). The extended coiled structures are located on the undersurface of the cytoplasmic membrane

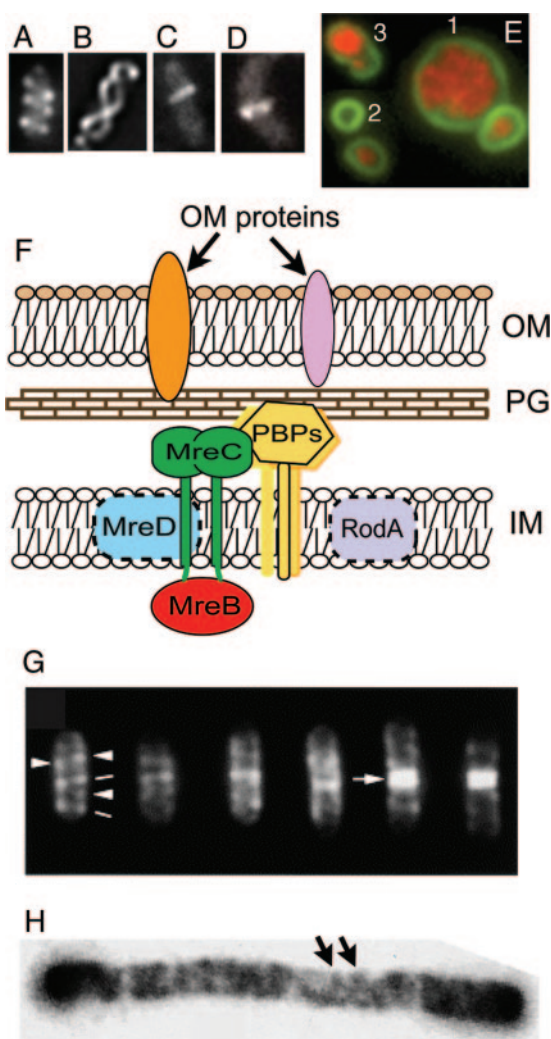


FIG. 2. Localization and functions of the actin-like MreB protein. (A to D) Cellular localization of MreB labeled with GFP or YFP. (A to C) *E. coli* MreB localizes into extended coils (A), intertwined double helices (B), and band-like structures (C). (Reprinted from reference 187 with permission of the publisher. Copyright 2003 National Academy of Sciences, U.S.A.) (D) *C. crescentus* MreB localizes into a band-like structure at the division site in predivisional cells. (Reprinted from reference 60 with permission of the publisher. Copyright 2004 National Academy of Sciences, U.S.A.) (E) Chromosome segregation in *E. coli mreB* deletion strain (Y.-L. Shih, unpublished). Defects include multiple disordered chromosomes and unequal chromosome partition into daughter cells (cell 1), production of anucleate cells (cell 2), and chromosome fragmentation presumably due to guillotining of the nucleoid (cell 3). Bacterial DNA (red) is stained with DAPI; membrane (green) is stained with FM4-64 [N-(3-triethylammonium-propyl)-4-(6-(4-(diethylamino)phenyl)hexatrienyl)pyridinium dibromide]. (F) Suggested organization of cytoskeleton-associated cell wall-synthesizing proteins of *E. coli*. The cytoplasmic MreB cytoskeleton is linked via MreC and MreD to the PBP murein biosynthetic enzymes (107). RodA may also be a member of the complex, and it is possible that some outer membrane proteins are also part of the MreC-associated structure (35). MreC is shown as a transmembrane protein (107, 113), but, at least in *C. crescentus*, MreC appears to be a periplasmic protein (35). See text for further details and references. This multi-protein structure may permit the MreB cytoskeleton to regulate the pattern of cell wall biosynthesis by providing spatial information to the murein biosynthetic machinery. OM, outer membrane; PG, peptidoglycan (murein); IM, inner membrane. (G) Pattern of murein assembly in *B. subtilis* (27). Nascent peptidoglycan was stained with

and frequently extend along the entire length of the cell. In some cases the structures consist of two intertwined helices (Fig. 2B).

The MreB helical cytoskeleton can change its cellular pattern, as implied by the observation that the helical density and cellular distribution of the MreB coiled structure varies in different cells within normally growing cultures (Fig. 2A to C) (53, 60, 95, 187, 191, 194). This is likely, at least in part, to reflect remodeling during the cell cycle. Thus, in *C. crescentus* the MreB helical arrays along the length of the cell are converted to a ring structure at or near midcell in predivisional cells (Fig. 2D) (53). In *R. sphaeroides*, a similar structure appears near midcell prior to cytokinesis and moves to another position before septation is completed (191). The redistribution event in *C. crescentus* did not occur when the essential cell division protein FtsZ was depleted, implying that formation of the MreB ring near midcell is regulated by cell division events (53). The formation of a ring-like structure near midcell in *C. crescentus* and *R. sphaeroides* is reminiscent of the formation of the actin contractile ring that is located at the division site in eukaryotic cells and plays a contractile role throughout cytokinesis in cooperation with myosin (4). However, aside from its transient midcell localization in several studies, there is no evidence that the MreB ring plays a role in bacterial cytokinesis. Similar band- or ring-like structures are present in about 5% of *E. coli* cells, without an apparent preference for localization near midcell (187), and the fact that  $\Delta mreB$  cells can undergo cell division shows that the MreB ring is not an essential element of the septation process (108, 188).

MreB redistribution into a ring structure near midcell in predivisional cells of *C. crescentus* is impaired, but not eliminated, in a strain that lacks TipN, a protein that normally marks the new cell pole and plays a role in establishment of the axis of cell polarity (83, 111). TipN overproduction leads to its mislocalization to ectopic positions along the cell cylinder, thereby establishing new axes of polarity as shown by outgrowth of rods as branches from the aberrant sites (111). It is possible that this reflects a direct influence of TipN on the directionality of the MreB cytoskeleton.

The MreB and Mbl cytoskeletal elements in *B. subtilis* are dynamic structures. Rapid movement has been observed within the GFP-labeled MreB and Mbl coiled structures, appearing sometimes to include segmental unidirectional movement detectable on a time scale of several seconds (194). Fluorescence photobleaching studies have also shown that molecules within the Mbl helical structure exchange with Mbl molecules elsewhere in the cell with a half time of approximately 8 min (20).

fluorescently labeled vancomycin (see the text). The micrograph contains cells representing different stages of the cell cycle. Helical patterns of labeled vancomycin are indicated by transverse bands (lines) and dots around the cell periphery (arrowheads). The densely stained bands (arrow) in the two right-most cells are located at the cell division sites. (Reprinted from reference 27 with permission from Elsevier.) (H) Pattern of murein insertion into the murein sacculus of *E. coli*, suggesting a helical mode of murein assembly (arrows indicate two of the helical coils). (Reprinted from reference 32 with permission of the publisher.)

**(ii) MreB polymerization and depolymerization.** The MreB protein of *Thermotoga maritima* self-assembles into long polymeric filaments in vitro (51, 214). Although the cellular abundance of MreB in *T. maritima* is not known, polymerization of *T. maritima* MreB is rapid at the normal cellular concentrations of *E. coli* MreB (~30,000 molecules per cell [108]) and *B. subtilis* MreB (~8,000 molecules per cell [95]). Each filament is composed of two side-by-side linear polymers that differ in appearance from the helical double-stranded filaments of F-actin (214). The double-stranded MreB filaments are likely to comprise the helical MreB structures of intact cells.

Polymerization occurs equally well in the presence of ATP and GTP (50, 214), thereby differing from actin polymerization, which occurs only in the presence of ATP. MreB polymerization stimulates ATPase activity, but during the course of MreB polymerization there is a lag between polymerization and phosphate release (50). This implies that ATP hydrolysis occurs after MreB monomers are incorporated into filaments and that ATP binding, rather than hydrolysis, is required for addition of subunits to the growing polymer, thereby resembling actin polymerization (164).

The filaments interact to form bundles that undergo a gelation process, leading to formation of a solid-like structure (51). The bundled MreB structure is more rigid than the equivalent F-actin structure, with properties that are more often associated with eukaryotic intermediate filaments than with actin (51). These include high elasticity, low critical concentrations for polymerization, and a high propensity for bundling. These properties would be useful if the MreB cytoskeleton played a true skeletal role in supporting cell shape. However, the significant changes in cellular distribution of the MreB cytoskeleton that take place within the rod-shaped cells (see above) indicate that the rigidity of organized MreB polymers does not play an essential role in maintaining the rod shape of the cell. This conclusion is supported by studies with the drug A22 [*S*-(3,4-dichlorobenzyl)isothioure] (88), which leads to loss of the MreB coiled structures and conversion of the cell from a rod to a sphere. When A22 was added, the rod-like shape of *C. crescentus* was not altered until long after disappearance of the MreB helical structures (61), arguing against the idea that rigidity of the bundled protofilaments is necessary for maintenance of cell shape.

All current information on the structure and polymerization properties of MreB filaments is based on studies of MreB from the thermophilic organism *T. maritima*, where the cellular organization of the protein has not yet been studied. Therefore, it will be important to confirm that MreB from organisms such as *B. subtilis*, *E. coli*, *Caulobacter crescentus*, and *Rhodobacter sphaeroides*, where almost all biological studies have been performed, behaves similarly to the *T. maritima* protein.

**(iii) Cellular functions of MreB and MreB homologs.** (a) *Cell shape determination.* Since the original discovery of the *mreB* (murein cluster B) gene in a search for mutants that are sensitive to amdinocillin (220), genes coding for MreB and MreB-related actin homologs have been shown to be present in almost all rod-shaped species and absent from species that grow as cocci (27). MreB-depleted cells usually grow as spheres, suggesting that MreB may play a role in cell shape control in rod-shaped bacteria.

It has long been known that the primary determinant of

bacterial cell shape is the murein (peptidoglycan) exoskeleton, which is located outside of the plasma membrane. The murein sacculus retains the shape of bacterial cells even when purified away from other cellular components, and in the absence of cell wall murein, rod-shaped cells become spherical. This makes it clear that the sacculus is the shape-determining structure of the cell (184). The *mreB* operon is part of a large cluster of genes involved in murein synthesis, implying a possible relation between MreB and biosynthesis of the rigid murein exoskeleton.

The shape of rod-shaped cells is dependent on enzymes responsible for longitudinal murein growth. The rod shape is also dependent on the presence of MreB or MreB homologs, since depletion of these proteins leads to loss of the normal rod shape, with formation of spherical cells, or, in the case of loss of Mbl, to markedly deformed cells with large bulges and irregular increases in cell width (95). It has been suggested that Mbl controls cylindrical cell wall synthesis (27). Several other cellular proteins are also implicated in establishment of the rod shape, since loss of these proteins also leads a rod-to-sphere transition. Among others, these include the murein biosynthetic enzyme penicillin-binding protein 2 (PBP2) and the RodA protein of *E. coli*, which are discussed below.

It is likely that MreB and its homologs regulate the shape of rod-shaped cells by organizing murein biosynthetic enzymes into a helical pattern that is oriented along the long axis of the cell, leading to the pattern of murein synthesis that is responsible for the rod shape. This was initially suggested by studies with fluorescein-labeled vancomycin. Vancomycin blocks the cross-linking of newly synthesized glycan-pentapeptide chains into the murein sacculus by covalently attaching to the terminal D-alanine of the pentapeptide murein biosynthetic precursors (12, 17, 27). Fluorescein-labeled vancomycin therefore has been used as a marker for the cellular pattern of murein biosynthesis. The vancomycin studies showed that the immediate precursors of mature murein in *B. subtilis* (27) are organized in a coiled pattern that extends along the long axis of the cell and resembles the distribution patterns of MreB and Mbl (Fig. 2G). The coiled vancomycin pattern was dependent on the presence of the MreB homolog Mbl (27). In species that lack an *mbl* gene, it is likely that MreB or another MreB homolog carries out this function. Consistent with these results, studies of murein deposition in *E. coli* cells (32) also suggest a coiled pattern of new murein incorporation into the sacculus (Fig. 2H).

The following experiments indicate that the Mbl-dependent helical pattern of murein synthesis reflects a helical organization of the murein biosynthetic enzymes needed for longitudinal cell growth. First, the biosynthetic murein transpeptidase PBP2, which is required for rod shape, is distributed in a coiled pattern along the cell cylinder, similar to the distribution patterns of MreB and Mbl. This has been shown in *C. crescentus* (35, 38, 53) and is likely also true in *E. coli* (30). Second, the coiled distribution pattern of PBP2 is dependent on the presence of MreB and MreC (35, 53), implying that the helical MreB and MreC cytoskeletal structures (discussed further below) play an essential role in determining the cellular organization of PBP2.

MreC appears to act as a bridge between the MreB cytoskeleton and the murein biosynthetic machinery, as shown in stud-

ies of *E. coli* and *B. subtilis* (107, 113). The MreD protein is also likely to be a component of the bridging complex in organisms that contain an *mreD* gene, such as *E. coli* and *B. subtilis*. Thus, *E. coli* MreC interacts with MreB and MreD in bacterial two-hybrid assays, whereas MreB does not interact with MreD (107). This suggests that MreC may be intercalated between MreB and MreD in a putative multiprotein complex. In addition, several lines of evidence suggest that MreB, MreC, MreD, PBP2, and perhaps other murein biosynthetic enzymes are components of a structure that mediates the effects of the MreB cytoskeleton on the topology of murein synthesis (Fig. 2F). First, formation of normal MreB helical cytoskeletal structures requires the presence of *mreC* and *mreD* in *E. coli* and *B. subtilis* (29, 107). Second, several PBPs which code for murein biosynthetic enzymes were recovered by affinity chromatography of a *C. crescentus* cell extract on an MreC column, suggesting a link between MreC and multiple elements of the murein biosynthetic machinery in this organism (35). Third, *C. crescentus* MreC and PBP2 (35, 38) and *B. subtilis* MreC and MreD (113) are present in helical patterns that resemble those of the MreB and Mbl coiled elements. It has been suggested that RodA, which is required for maintenance of the rod shape and for the enzymatic activity of PBP2 (87, 196), may be another component of the MreBC complex (107). MreC has been thought to be the transmembrane link in this complex (107), because sequence analysis predicts a transmembrane organization. However, it has recently been reported that cell fractionation studies indicate a periplasmic location for the *C. crescentus* MreC protein (35). Further studies will be needed to clarify the cellular location of MreC in the various organisms under study.

The interaction between MreB and the MreC-based structure *in vivo* appears to be transient, since, in contrast to MreB, the distribution of the MreC helical pattern does not significantly change during the cell cycle (35). The observation that disruption of the MreB helical structures by A22 did not have immediate effects on the localization of MreC and PBP2 also supports the idea that MreB is not an essential part of the basic MreC-PBP complex (35, 38).

MreC affinity chromatography identified approximately 19 candidates to be MreC-associated proteins (35). These included eight presumed outer membrane proteins, nine cytoplasmic proteins, and small amounts of several PBPs. Studies of GFP derivatives of five of the outer membrane proteins showed clusters of labeled protein that were interpreted to indicate a spiral, punctate, or banding distribution pattern similar to that seen with MreC and PBP2 (35). Based on these results, it was suggested that the PBPs and outer membrane proteins might be part of an MreC-based complex anchored in the inner membrane that could provide a link between the internal MreB cytoskeleton and the outer layers of the cell envelope. If this is correct, the failure to recover MreB from the MreC affinity column might be attributed to problems in solubilization of the MreB cytoskeletal structures or to the presence of intermediate linking proteins between MreB and MreC. Further work will be needed to fully interpret these observations.

Interestingly, loss of either MreB or MreC causes PBP2 to lose its helical organization and instead to localize near midcell in *C. crescentus* (38). This requires the essential division pro-

tein FtsZ, suggesting that the cellular localization of PBP2, and presumably also its site of action, may be regulated by an interplay between the cell division machinery and the MreB/MreC cytoskeleton. This is consistent with the observation that PBP2 localizes to midcell at the time of septation in *E. coli* (30). The unrelated PBP2 of *Staphylococcus aureus* also localizes to midcell (161).

A full understanding of the role of the cytoskeleton in organizing the murein biosynthetic machinery is complicated by observations such as the following. (i) Localization studies of all 11 vegetative PBPs of *B. subtilis* failed to show a helical distribution (182). Unless these results reflect technical limitations, this implies that the association of murein biosynthetic enzymes with the cytoskeleton may vary from species to species or may be limited to a small subset of the enzymes. (ii) Growth of *B. subtilis* in the presence of 25 mM  $Mg^{2+}$  restored a normal rod morphology and normal helical distribution of nascent murein to  $\Delta mreB$  cells (54). Therefore, although there is inferential evidence that the MreB cytoskeleton may participate in determination of cell shape by providing a scaffold for the helical distribution of murein biosynthetic enzymes along the length of the cell, this effect either is indirect or operates through another scaffolding protein, perhaps MreC. High  $Mg^{2+}$  levels could stabilize the scaffolding partner to permit it to function in the absence of MreB. These observations show that the MreB cytoskeleton is not essential for cell shape determination in *B. subtilis* despite the fact that depletion of MreB results in a change of cell shape.

(b) *Cell polarity*. The poles of rod-shaped cells differ in several respects from the remainder of the cell body. These differences include the specific polar localization of a number of membrane-associated proteins (90), the presence of polar flagella or pili in certain species (185), the lack of turnover of murein and of externally labeled surface proteins at the cell poles (31, 33), the absence of zones of adhesion between the inner membrane and the murein-outer membrane layer at the poles (23, 131), and anatomic changes (the bacterial birth scar) at the newly formed cell pole (130). MreB has been implicated in one of these aspects of cell polarity, the localization of specific proteins to one or both cell poles.

Proteins that play a role in regulating the *C. crescentus* differentiation cycle are differentially targeted to one or both cell poles (reviewed in reference 59). These include the membrane histidine kinases, PleC, DivJ, and CckA. MreB is required for the polar targeting of these proteins (60). After depletion of MreB, polar localization of the proteins is lost and they become diffusely distributed within the cell.

MreB is also required for the polar localization of proteins in other organisms. In *E. coli* and related gram-negative bacteria, membrane-associated proteins involved in chemotaxis, motility, secretion, and virulence are normally targeted to one or both cell poles (185). When several of these proteins were expressed in *E. coli*, depletion of MreB led to a change of polar targeting. The proteins include the *E. coli* aspartate chemoreceptor (188), the *Shigella flexneri* virulence protein IcsA (151, 188), and the *Vibrio cholerae* type II secretion protein EpsM (151). It is likely that MreB also will be shown to play a role in the polar targeting of other proteins.

However, not all polar proteins require MreB for their localization. Thus, the assembly of the *E. coli* Min proteins into

membrane-associated polar zones (188, 205) and the polar localization of the *C. crescentus* TipN protein (111) appear to be independent of MreB. These may be exceptions to the general rule that MreB is involved in localization of polar proteins, reflecting the special role that the Min proteins play in establishing the position of the cellular division site (175) and the special role of TipN in marking the cell pole and in determination of cell polarity (83, 111). It is not known how MreB accomplishes the polar targeting of proteins. The MreB helical filaments could participate directly in moving the proteins to the poles by providing tracks for the active translocation of specific cargo proteins, probably in collaboration with substrate-specific carrier and/or motor proteins. Segments of the MreB filaments might themselves move toward the poles (194) as part of the translocation process. Alternatively, MreB might act indirectly by positioning polar targets for protein localization. For example, the polar end of the MreB cytoskeleton might initiate the localization or organization of other polar components that would then act as polar binding sites for a family of substrate proteins. The targets need not be proteins, since both the specialized membrane lipid composition of the poles (141) and the presence of a segregated polar murein compartment (33) could contribute to the target sites.

(c) *Chromosome segregation.* During the normal cell cycle, daughter nucleoids move rapidly to opposite ends of the cell, leading to their equipartition into the two daughter cells (74). This process is perturbed when MreB is depleted in *E. coli* and *C. crescentus* (60, 108). This is manifested by the production of cells in which multiple nucleoids are irregularly distributed within the cytoplasm (Fig. 2E, cell 1) (108) and of anucleate cells (Fig. 2E, cell 2) or cells in which an incompletely partitioned nucleoid is guillotined by the septum (2E, cell 3). The possibility that the nucleoid segregation defects are caused by the spherical shape of the MreB-depleted cells has been excluded by the observation that expression of certain mutant alleles of *mreB* that do not interfere with the rod shape of the cell is still associated with nucleoid segregation defects (106, 108).

Further evidence that MreB is needed for normal chromosome partition came from studies of the segregation of the origin and terminus regions of newly replicated chromosomes of *E. coli* and *C. crescentus* (61, 108). In wild-type cells, the newly replicated *oriC* regions rapidly move to opposite ends of the cell. Separation of the terminus regions takes place later. In contrast, in MreB-depleted cells, the normal movement of the newly replicated *oriC* regions to opposite ends of the cell does not occur, and the terminus regions appear to adhere together (106, 108).

Biochemical evidence that the *oriC* region is the chromosomal target of MreB came from studies of *C. crescentus* cell extracts by Gitai and coworkers showing that MreB and DNA from the origin-proximal region could be chemically cross-linked and were coimmunoprecipitated with anti-MreB antiserum (61). This strongly implies that MreB is associated with the origin-proximal region of the chromosome, either directly or via other proteins that correspond to the centromere-binding kinetochore proteins of eukaryotic cells. These results imply that the association of the MreB cytoskeleton with the *oriC* region plays an important role in moving the daughter chro-

mosomes towards opposite cell poles.

The mechanism responsible for the chromosomal movement is not known. Based on the present evidence, it appears likely that the *oriC* region directly or indirectly interacts with the MreB cytoskeleton and is then translocated along the helical MreB structures from midcell to the cell poles, perhaps accompanied by movement of segments of the MreB filaments (194). The energy requirement for translocation could be met by a separate motor protein, by coupling the ATPase activity of MreB to movement of the DNA, or by changes in chromosome folding. It is not known whether active movement of other chromosomal regions by a similar translocation mechanism is also involved in the segregation process. This may not be needed, since the active compaction of chromosomal DNA after *oriC* is moved to the poles could complete the process of nucleoid separation (147, 181). It also is not known whether the redistribution of MreB that occurs during the cell cycle is related to the *oriC* translocation events (53, 191).

The previous suggestion that RNA polymerase (RNAP) contributes to the motive force for chromosome separation (37) is supported by the recent finding that inactivation of RNAP in *E. coli* leads to a defect in nucleoid separation in DAPI (4',6'-diamidino-2-phenylindole)-stained cells, similar to the effect of MreB depletion or inactivation (106). This appears to be primarily associated with a failure of the terminus regions to segregate, although there may also be some effect on origin segregation. Of special interest, immunoprecipitation experiments using anti-MreB antibody indicated that MreB and RNAP are physically associated in cell extracts and in *in vitro* reconstitution experiments (106). These results suggest that RNAP is associated with the MreB cytoskeleton and works together with MreB in the chromosomal segregation process. It has been pointed out that a significant force can be generated by a stationary RNAP molecule during transcription, and this could contribute to moving DNA during the segregation process (37, 56).

A mechanism must also exist to explain the vectorial nature of the translocation process, in which the two newly replicated *oriC* regions are moved to opposite ends of the cell. The directionality could be provided by a double-helical MreB cytoskeletal structure (Fig. 2B) if the helical strands were of opposite polarity. This would provide two tracks that point in opposite directions, each providing a one-way highway for the *oriC* cargo. In another model the directionality would be imparted by the orientation of the newly replicated *oriC* regions as they exit from the replication apparatus (37). The two models are not mutually exclusive, and other mechanisms are also possible. A fuller understanding of the role of the MreB cytoskeleton in chromosome segregation will require a more detailed understanding of the macromolecular organization of the MreB helical arrays, the polarity of filament assembly and disassembly, and the basis of the MreB-*oriC* interaction. In contrast to the results for *E. coli* and *C. crescentus*, it is not clear whether MreB or one of the other actin homologs, Mbl or MreBH, is required for chromosome segregation in *B. subtilis* (54, 193). Thus, depletion of MreB in *B. subtilis* in the absence of polar effects on downstream genes did not lead to significant defects in chromosome segregation (54), and depletion of MreB or Mbl led to only mild segregation defects (194). Whether the third *B. subtilis* actin homolog, MreBH, influ-

ences chromosome segregation remains to be determined. It also will be of interest to see what mechanism is used for chromosome segregation in coccidial species, which lack MreB homologs.

#### Plasmid partitioning by an actin homolog: the ParM system.

Stable inheritance of low-copy plasmids is carried out by active partitioning systems that include a partitioning protein with ATPase activity. In type I partitioning systems these proteins belong to the Walker-type ATPase superfamily, and these are discussed later in this review. In type II systems the partitioning protein is an ATPase belonging to the actin protein superfamily, exemplified by the ParM protein of *E. coli* plasmid R1.

The *par* locus of plasmid R1 is the best-understood example of a bacterial system that fulfills the role of the mitotic apparatus of eukaryotic cells. The locus includes three genes: *parM* codes for the actin-like ParM protein (*M* for motor); *parC* is the *cis*-acting centromeric DNA site (*C* for centromere); and *parR* (*R* for repressor) codes for the ParR protein, which binds to *parC* sequences and acts both to autoregulate transcription of the *par* genes and to link the ParM motor protein to the plasmid DNA. The *parC* site contains 10 iterons of 11-base-pair repeats that act as sites for ParR binding (93).

In plasmid-containing cells, ParM forms linear filamentous structures that extend along the long axis of the cell, where they can be visualized by immunofluorescence microscopy (Fig. 3A, panel 1) (145, 146). The high cellular abundance of ParM (~18,000 molecules per cell) suggests that each intracellular filament consists of a number of protofilaments (145, 146). Growth of the ParM filaments pushes the progeny plasmids to opposite ends of the cell (Fig. 3B), as discussed below.

(i) **ParM polymer assembly and disassembly.** ParM polymerizes *in vitro* to form filaments that presumably correspond to the intracellular ParM filaments. Each *in vitro* filament is a double-stranded helical structure in which each helical strand is presumably a single ParM polymer. Unlike actin and MreB filaments, ParM filaments do not form bundles or sheets *in vitro* (55, 214, 216).

ParM filament assembly and disassembly are regulated by ATP binding and hydrolysis (55, 145, 146). Filament assembly requires either ATP or a nonhydrolyzable ATP analog, indicating that the ATP-bound form of ParM is competent to polymerize (55, 93, 146). Unlike actin filaments, in which subunits are added only at one end of the filament, ParM filaments grow by addition of subunits at both ends of the growing polymer (55).

Polymer growth occurs by addition of a ParM-ATP subunit to the end of the ParM chain. This is associated with hydrolysis of the ATP moiety of the previously incorporated terminal ParM-ATP, explaining the polymerization-dependent ATPase activity of the system. This generates ParM-ADP as the new penultimate residue of the polymer (Fig. 3C). Thus, ParM filaments consist of chains of ParM-ADP, capped by the most recently added ParM-ATP subunits. ParM-ADP polymers are very unstable and have a high probability of disassembly unless capped by ParM-ATP (55).

A dramatic feature of the *in vitro* ParM polymerization system in the absence of ParR-*parC* is the sudden switch after a variable period of bidirectional elongation to a stage of rapid catastrophic disassembly from one end of the filament, presumably triggered by an increase in the rate of hydrolysis of the

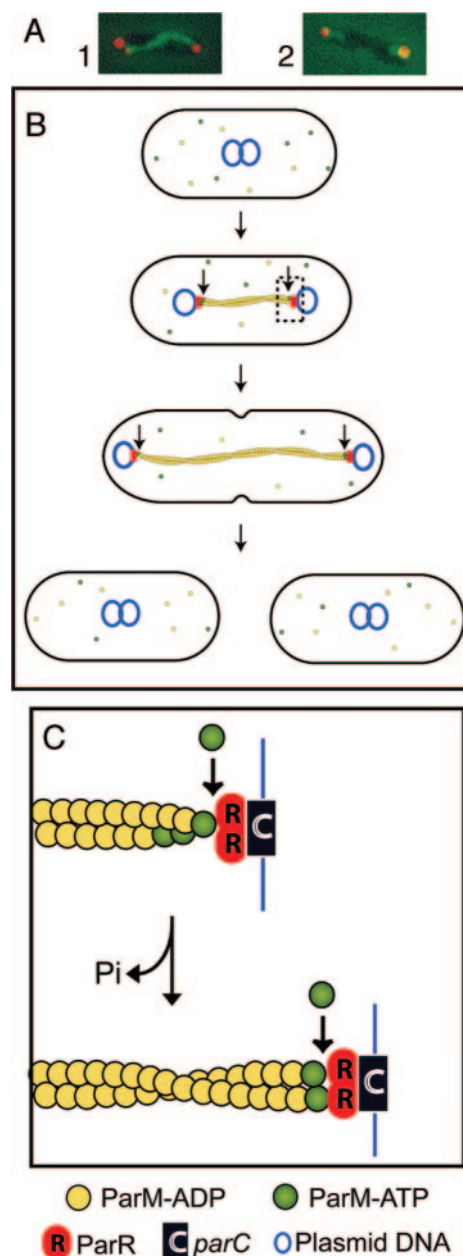


FIG. 3. ParM-mediated partition of plasmid R1. (A) Fluorescence micrographs showing the ParM filament (green) and plasmid DNA (red). Panel 1 shows a ParM filament extending between two plasmids that are located at the ends of the cell. Panel 2 shows a plasmid at each cell pole, attached to a short ParM filament that extends toward midcell; this presumably represents an intermediate stage of filament disassembly after the plasmids have been delivered to the ends of the cell. (Reprinted from reference 145 with permission from Elsevier.) (B) After plasmid replication, growth of a ParM polymeric filament (yellow) pushes apart the two progeny R1 plasmids, moving them from midcell to the two poles. (C) Cartoon representing the boxed region in panel B, showing details of the addition of new subunits at the two ends of the ParM filament. The ParM-ADP filament is capped by ParM-ATP subunits. The capped end is attached to the *parC* centromeric region of the plasmid via the ParR protein. ParM filament growth occurs by insertion of ParM-ATP subunits at the interface between the end of the ParM filament and the ParR/*parC* complex. This is associated with hydrolysis of the ATP moiety of the previous ParM-ATP subunit, thereby converting the penultimate subunit to ParM-ADP.

terminal ATP of the polymer (55). This reflects the fact that although the rate of subunit addition at the ends of the ParM filament is similar to the rate of growth of actin filaments, the rate of disassembly is 100 times higher than that of F-actin (55). A similar pattern of dynamic instability is characteristic of eukaryotic microtubules. The dynamic instability is thought to be necessary to prevent intracellular ParM filaments from growing to significant lengths before they interact with their plasmid targets (55).

**(ii) Mechanism of ParM function.** A substantial body of evidence indicates that ParR acts as a bridge between the ends of the ParM filament and the plasmid DNA that will be moved to the ends of the cell (Fig. 3B and C) (92, 94, 145, 146). Plasmid R1, like other unit copy plasmids, is replicated near midcell. ParR protein dimers then interact with the 10 iterons in the *parC* domains of the two daughter plasmids, leading to formation of plasmid pairs held together by multiple copies of ParR (94). The ends of a ParM oligomer or short polymer (55) then interact with the ParR-*parC* complex, separating the plasmid pair and leaving each end of the filament bound via ParR to a molecule of plasmid DNA (Fig. 3B). The polymer then grows bidirectionally by addition of new ParM subunits that are inserted between the end of the ParM filament and its ParR-*parC* cap, thereby pushing the two attached plasmids toward opposite ends of the cell (Fig. 3B and C). Addition of each new subunit is thought to be accompanied by hydrolysis of the ATP of the terminal ParM-ATP cap (Fig. 3C), as discussed above.

The presence of the ParR-*parC* complexes at the two ends of the ParM filament inhibits the dissociation of subunits during the period of polymer growth, preventing the catastrophic disassembly that otherwise would occur after a relatively limited period of polymer growth (55). Polymer growth stops when the ends of the filament approach the ends of the cell. The expected intermediate structure, a filament extending along the long axis of the cell with plasmid DNA attached at both ends, has been visualized in elegant double-label studies by Møller-Jensen et al. (Fig. 3A, panel 1) (145). The ParM polymers then disassemble, providing ParM subunits for initiating the cycle of filament assembly that will occur after plasmid replication at the midcell replication site in the daughter cell.

**(iii) Filament disassembly and plasmid migration.** The mechanism responsible for triggering disassembly of the ParM filament is not yet understood. We consider two possible modes of filament disassembly. (i) Disassembly proceeds bidirectionally from the two ends of the intact filament in response to a signal related to the arrival of the plasmids at the cell poles. To achieve this, the assembly/disassembly balance must be changed to favor disassembly from the ends of the filament. The switch from polymer growth to polymer disassembly may reflect a decrease in the rate of subunit addition as a consequence of low cytoplasmic ParM concentration resulting from its incorporation into the growing polymer as well as a diminution in synthesis of ParM because of the transcriptional autoregulation of the operon (41). This is likely to be associated with release of the ParR-plasmid complex, which normally inhibits subunit loss. It should generate cells containing a single ParM filament with two free ends. The filament will become progressively shorter as subunits are released from both ends. Although the predicted interme-

diate structures have not been detected, this could be explained if disassembly was too rapid for easy detection or if the stochastic disassembly of protofilaments left some individual pole-to-pole protofilaments intact through much of the disassembly period. (ii) In a second model, disassembly proceeds from midcell to each of the cell poles, initiated by internal cleavage of the filament. This would generate two filaments, each with a free end located somewhere near midcell and a plasmid-ParR complex at its polar end. Because the free ends lack a ParR-*parC* cap, the two filaments will disassemble rapidly from the free ends toward the cell poles. Cleavage might be carried out by proteins similar to eukaryotic factors that sever microtubules and actin filaments, such as katanins and cofilins, respectively (132, 137). Consistent with this model, the predicted intermediate structures, short ParM filaments each extending toward midcell from a plasmid located at a cell pole, have been visualized in double-label experiments (Fig. 3A, panel 2). At this point it is not possible to make a definitive choice between these two alternative disassembly mechanisms, each of which would presumably leave the plasmids in opposite ends of the cell.

The mechanism of movement of the segregated plasmids from the ends of the cell to their new replication sites has not been defined. After the ParM filament is disassembled, each released plasmid must move from the end of the cell to the new replication site, which will be located at midcell in the postdivision cell. During this process the freed plasmid must be prevented from diffusing back into the other half of the cell prior to septal closure. Although it is not known how this is accomplished, there are several possibilities. (i) The initiation of polymer disassembly could be coupled to an event in the cell cycle to ensure that the ParM filaments would not start to disassemble before septation occurred. (ii) A segregation trap could be present at the cell quarters to trap plasmids released at the proximal cell pole. The trap could, for example, be provided by the newly assembled plasmid replication machinery. This would require the replication apparatus to assemble at the cell quarters prior to septum formation at midcell, perhaps at the same positions where the cell division machinery assembles in rapidly growing cells (176). A plasmid diffusing from the proximal pole would encounter and engage with this site before crossing midcell. (iii) Cleavage of the ParM filament and subsequent disassembly of the filament (according to the second model in the paragraph above) could be directly or indirectly dependent on septation, consistent with the observation that ParM filaments do not disassemble when septation is blocked by cephalixin treatment (Fig. 2Ar in reference 146). This would ensure that plasmid release and diffusion from the pole would not occur until after septation occurred. In a simple model, filament cleavage could be a direct result of septum formation. Cleavage proteins might even be present at the leading edge of the ingrowing septum, where other functional proteins are located (48). (iv) The plasmids could associate with specific polar binding sites until a signal for their release is received. All of the above mechanisms, except for mechanical disruption of the ParM filament by the ingrowing septum, would require host cell factors.

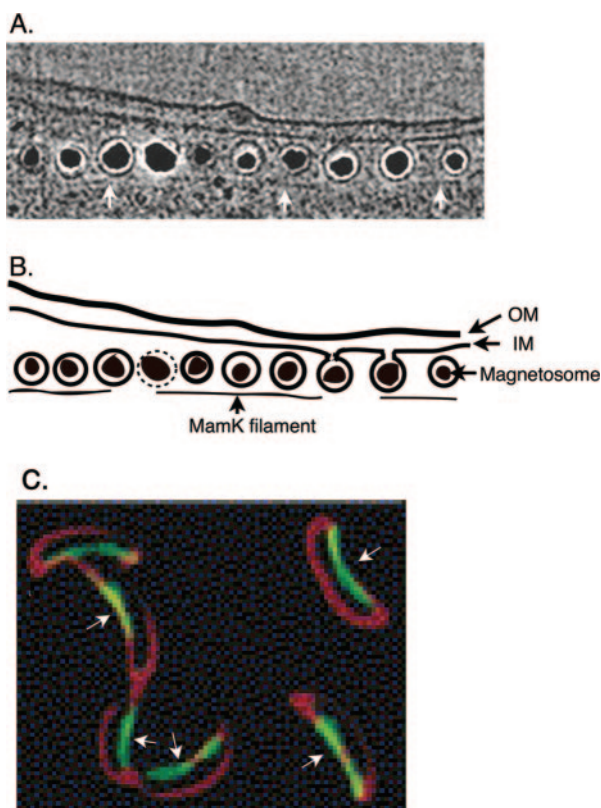


FIG. 4. Intracellular cytoskeletal structures formed by the actin-like MamK protein (A and B) and the intermediate filament homolog crescentin (C). (A and B) Electron cryotomography (A) and cartoon illustration (B) of magnetosomes located under the surface of the cytoplasmic membrane of *Magnetospirillum magneticum*. MamK filaments extend along the surface of the linear array of membrane-bounded magnetosome structures (white arrows in panel A). (The electron micrograph was reprinted from reference 101 with permission of AAAS.) (C) The intermediate filament-like protein crescentin (green), visualized by expressing GFP-tagged crescentin in wild-type cells, forms filamentous structures (white arrows) along the concave edge of *C. crescentus*. Membranes (in red) are stained with dye FM 4-64. (Reprinted from reference 8 with permission from Elsevier.)

**MamK.** MamK is an actin homolog that plays a role in the subcellular organization of magnetosomal membranes. This defines a new function of actin-like proteins, the positioning of cellular organelles in bacterial cells (101).

Magnetosomes are membrane-bounded organelles of *Magnetospirillum magneticum* sp. strain AMB01 that contain iron crystals within the membrane-bounded structures. Electron cryotomography has shown that the magnetosomal membranes represent membrane invaginations of the cytoplasmic membrane which are organized into linear arrays that are generally oriented along the long axis of the cell (101). The magnetosomes are bordered by filamentous MamK structures that extend along the length of the organellar structures near the inner curvature of the cell (Fig. 4A and B) (101). They have been visualized by electron cryotomography and by labeling cells with MamK fused to GFP. Deletion of *mamK* leads to both disappearance of the filaments and disappearance of the ordered magnetosome membrane arrays, confirming that the

MamK cytoskeleton-like structures are required for magnetosome organization within the cell.

### Tubulin Homologs

Two types of tubulin homolog, exemplified by FtsZ and the BtubA and BtubB proteins of *Prostheco bacter de j ongeii*, have been identified in prokaryotes. FtsZ, BtubA/B, and eukaryotic tubulins form a distinct family of GTPases (152, 183). The three-dimensional structures of the bacterial tubulin homologs are similar to the structure of eukaryotic tubulins (Fig. 1B), although sequence homology between the bacterial proteins and tubulins varies considerably (sequence identities of 17% for FtsZ and 35% for BtubA/B relative to eukaryotic tubulin [123, 183]).

Phylogenetic analysis suggests that FtsZ and tubulin are likely to have evolved from a common ancestor and to have diverged at an early stage of evolution, whereas BtubA and BtubB have evolved more recently following horizontal gene transfer of a tubulin or tubulin-like gene from a eukaryotic parent (91, 183, 192, 195). Consistent with this suggestion, BtubA and BtubB are more similar to tubulin than to FtsZ in amino acid sequence and protein structure, whereas other *P. de j ongeii* genes are considered phylogenetically closer to their prokaryotic counterparts (91, 195). BtubA contains a carboxyl-terminal domain that resembles the carboxyl terminus of tubulin and is missing in FtsZ. This domain is important for the interaction of tubulin with motor proteins and tubulin-associated proteins.

**FtsZ.** FtsZ is essential for bacterial cytokinesis, and highly conserved FtsZ homologs are present in almost all bacteria and archaea. FtsZ homologs are also present in eukaryotic organelles such as plastids, which are believed to be derived from bacterial endosymbionts (for a review, see reference 5). A plasmid-borne FtsZ variant that plays a role in plasmid replication is also found in virulence plasmid pXO1 of *Bacillus anthracis* (155, 156) and in other megaplasmids (207). The role of FtsZ in cellular and organelle division has recently been reviewed (47, 133, 172).

**(i) The FtsZ ring.** FtsZ is an essential cell division protein in most bacteria. It is the earliest known component of the division machinery to be targeted to the cell division site, where it assembles into a circumferential ring, the Z-ring, located at the inner surface of the cytoplasmic membrane (Fig. 5D). The Z-ring has been visualized by immunoelectron microscopy (15) and by fluorescence microscopy using anti-FtsZ antibody or FtsZ linked to GFP or one of its derivatives (Fig. 5A) (3, 129). The Z-ring is believed to consist a number of polymeric FtsZ protofilaments, but it is not known whether individual protofilaments extend completely around the cell circumference or whether there are larger numbers of shorter polymers that extend around the cell in some type of staggered configuration.

The *E. coli* Z-ring acts as a scaffold for assembly of at least 10 additional proteins into a cytokinetic ring (also called the septosome or divisome) (Fig. 5D) (63). Formation of the cytokinetic ring is followed by ingrowth of the septum after a variable delay. Although FtsZ remains associated with the inner edge of the ingrowing septum as septal invagination progresses, it is not known whether the Z-ring plays a direct role in the constriction process. In addition to its role in as-

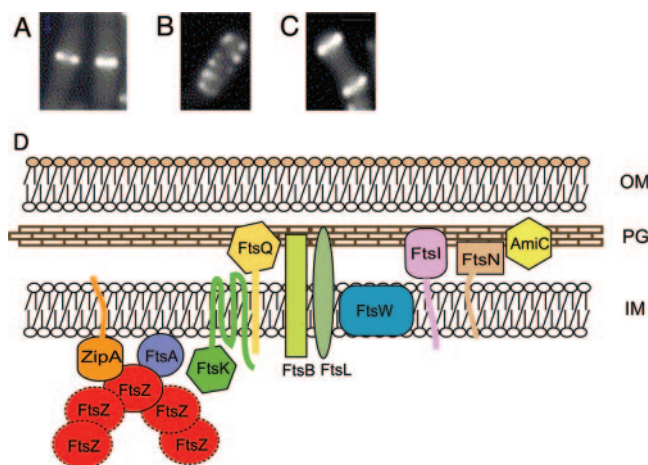


FIG. 5. Cellular organization of FtsZ. (A to C) Immunofluorescence micrographs showing cellular localization of FtsZ in *B. subtilis* cells. (Reprinted from reference 13 with permission from Elsevier.) (A) FtsZ ring at midcell during vegetative growth; (B) extended FtsZ helical structures during the transition from vegetative growth to sporulation; (C) bipolar FtsZ rings at a later stage of the transition. (D) Diagrammatic representation of a portion of the cytokinetic ring (septasome) of *E. coli*. FtsZ is anchored to the cell membrane by FtsA and ZipA, and the other septasomal proteins are then added to the complex (63). The symbols representing the proteins are arranged for clarity, and the cartoon does not accurately represent the details of their interactions. OM, outer membrane; PG, peptidoglycan (murein); IM, inner membrane.

sembling the cytokinetic machinery, FtsZ may also play a role in the cell cycle-dependent switch from longitudinal murein synthesis to the synthesis of preseptal murein at the future division site (34, 174). The intact Z-ring and cytokinetic ring have not yet been isolated, and the details of their structures are not known.

FtsZ is a high-abundance protein (reported to be present at 3,400 to 20,000 copies per *E. coli* cell) (26, 125, 149, 162, 178, 197). Of the other components of the cytokinetic ring, FtsA and ZipA are present at approximately 740 and 1,250 copies per cell, respectively (66, 178), whereas the other ring components are much less abundant, at 30 to 50 molecules per cell (176). The components of the septasome carry out a variety of functions in the septation process, most of which are poorly understood.

Interestingly, studies using fluorescence recovery after photobleaching have shown that the Z-ring is a highly dynamic structure, with FtsZ molecules exchanging with FtsZ molecules elsewhere in the cell with a half time of  $\leq 30$  seconds, depending upon experimental conditions (6, 197). It is not known whether the exchange of FtsZ molecules occurs along the length of the polymer or only at the ends of FtsZ polymers. Atomic force microscopy has indicated that FtsZ polymers undergo fragmentation and reannealing at internal locations (143). Therefore, it is possible that the exchange occurs at internal sites within FtsZ polymers, accompanied by the repeated breaking and resealing at internal sites within polymer strands. The potential for breaking and resealing of the polymer could also provide a mechanism for extrusion of FtsZ molecules during the shrinkage of the Z ring that occurs during septal constriction.

**(ii) Membrane attachment of the Z-ring.** Assembly of the Z-ring of *E. coli* requires the FtsA or ZipA protein to anchor the Z-ring to the membrane and possibly also to promote ring assembly or stability. Either protein is sufficient to support membrane association of FtsZ and formation of the Z-ring. Interestingly, although either FtsA or ZipA is capable of supporting Z-ring formation, both proteins are required for the subsequent entry of the other division proteins into the ring (63), and FtsZ, FtsA, and ZipA all remain as permanent components of the cytokinetic ring. FtsA homologs are found in many bacterial species, whereas ZipA is restricted to a small number of organisms. It is not known whether different proteins in other species fulfill the role of the *E. coli* ZipA protein.

ZipA contains a single hydrophobic transmembrane domain that anchors the Z-ring to the membrane (160). In contrast, FtsA anchors the Z-ring to the membrane via an amphipathic helix at the carboxy terminus of the FtsA protein, with the hydrophobic amino acid side chains on the nonpolar face of the helix inserting into the interior of the membrane bilayer (159). A similar amphipathic helix is present at the carboxyl termini of FtsA proteins of other species. The amphipathic helical membrane-binding domain of FtsA is similar in structure to and is interchangeable with the membrane-binding domain of MinD (159) (discussed below), demonstrating the relatively nonspecific nature of the membrane anchor. It is not known whether the Z-ring formed in the absence of one of the two anchoring proteins is structurally identical to the Z-ring formed when both membrane-binding proteins are present or whether FtsA and ZipA perform roles in the division process other than their roles in Z-ring anchoring and septasome assembly.

FtsA is an actin homolog, as shown by sequence and structural similarities (16, 215). The *Streptococcus pneumoniae* FtsA protein polymerizes in vitro in the presence of ATP (112), and removal of the *E. coli* membrane-targeting sequence is associated with formation of FtsA filaments within the cytoplasm (159). The ability of cytoplasmic FtsA to form polymeric filaments in vitro and the formation of FtsA filaments in *E. coli* suggest that FtsA may play a cytoskeleton-like role in the structure of the cytokinetic ring or in the septation process itself, in addition to its role in anchoring FtsZ to the membrane.

**(iii) FtsZ spiral structures.** In addition to constituting the Z-ring at division sites, FtsZ also forms transient helical arrays that coil around the long axis of the cell, resembling the helical structures formed by cytoskeletal proteins MreB, Mbl, MreBH, and MinD.

Evidence suggesting that the FtsZ spiral structures may be intermediates in formation of the FtsZ ring has come from studies of sporulating and vegetative *B. subtilis* cells (13). During sporogenesis the septation site switches from midcell to a site near one pole, requiring repositioning of the Z-ring from its normal midcell location. During this process, disappearance of the midcell ring is followed by the appearance of new Z-rings at both cell poles (Fig. 5C). One ring then disappears, and the other progresses to assemble the division machinery for formation of the polar spore septum (119). Ben Yehuda and Losick have shown that spiral FtsZ structures extend along the long axis of the cell during the change from medial

to polar Z-rings (Fig. 5B), suggesting that these represent intermediates in the FtsZ redistribution process during sporogenesis (13).

Studies of a thermosensitive FtsZ mutant suggested that FtsZ spiral structures may be intermediates in formation of the FtsZ ring in vegetatively growing as well as sporulating *B. subtilis* cells (140). When grown at the nonpermissive temperature, FtsZ rings did not form and were replaced by short FtsZ spiral structures located in internucleoid regions along the cell. On shift back to permissive temperature, time-lapse microscopy of FtsZ-YFP showed rapid conversion of the spirals to Z-rings. On the basis of these observations it was suggested that the mutation causes a block in conversion of FtsZ spirals to FtsZ rings, implying that the spiral structures are precursors of the Z-ring.

The structural relationship between FtsZ spirals and Z-rings has not been established. The two structures may be independent, with FtsZ molecules leaving the spiral to form a ring structure at the division site. On the other hand, it is quite possible that the Z-ring is not a true ring but rather a tightly compressed spiral structure derived from the more extended FtsZ helical structures discussed above. A choice between these alternatives will require higher-resolution studies of Z-rings within cells and/or the isolation and characterization of the Z-ring itself.

It also has been shown that FtsZ helical structures are present in *E. coli* cells that overproduce FtsZ or FtsZ-GFP, a protein that is not fully functional but that is used as a marker for Z-rings and other FtsZ structures in living cells (129, 199). The coiled FtsZ arrays show periodic waves of oscillation with a periodicity of 30 to 60 s (205). This oscillatory behavior was unaffected by loss of the MreB helical cytoskeleton, but the periodicity was interrupted in a *minCDE* deletion mutant, in which division site placement is perturbed (205). The relationship of these observations to the behavior of the Min proteins, which are required for identification of the division site and which also are organized into oscillating helical structures (discussed below), remains to be defined.

**(iv) FtsZ polymerization and depolymerization.** The three-dimensional structure of FtsZ from *Methanococcus jannaschii* resembles the structures of  $\alpha$ - and  $\beta$ -tubulins (Fig. 1B). There also are similarities in the polymerization characteristics of FtsZ and tubulins. In both cases the proteins polymerize unidirectionally into linear protofilaments in a GTP-dependent manner. Under appropriate conditions, the FtsZ and tubulin filaments both form bundles and sheets (45, 123). Rheometric measurements have indicated that bundles of FtsZ polymers form highly elastic structures, and it was suggested that this could be useful in maintenance of the Z-ring under the pressures generated during septal constriction (52).

However, there is no evidence that FtsZ forms microtubular structures in vitro or in vivo, and there are significant differences in the kinetics of nucleotide exchange between FtsZ and tubulin filaments. There also is no convincing evidence that FtsZ filaments are composed of FtsZ-GDP polymers capped with an FtsZ-GTP subunit whose hydrolysis leads to rapid polymer disassembly, as is the case for tubulin polymers. Instead, the polymer appears to consist of FtsZ-GTP subunits, and FtsZ polymer disassembly in vitro appears to be regulated by a balance between the rates of GTP hydrolysis and GTP

TABLE 1. Positive and negative regulators of FtsZ ring formation

Regulator	Function (reference[s])
<b>Positive</b>	
FtsA .....	FtsZ membrane anchor (159)
ZipA .....	FtsZ membrane anchor (66, 67, 169)
ZapA .....	Promote FtsZ ring stability (64)
<b>Negative</b>	
MinC .....	Position of FtsZ ring (28, 75, 96)
EzrA .....	Inhibit FtsZ ring formation (65, 118)
SulA .....	SOS response division inhibitor (73, 80, 96, 148, 211, 212)
SlmA .....	Inhibit FtsZ ring formation over nucleoids (14)

rebinding to FtsZ along the length of the filament (82, 133, 142, 157, 172). This conclusion is based on the observation that hydrolysis of bound GTP leads to disassembly of FtsZ filaments unless sufficient GTP is available to exchange with the GDP product (reviewed in reference 172). Although changes in GTP/GDP ratio affect the rate of polymer disassembly, it is unlikely that this could explain the loss of FtsZ subunits from the Z-ring during septal constriction, because the high GTP/GDP ratio in the cytosol should provide sufficient GTP to prevent spontaneous filament disassembly. The important question of the mechanism whereby the Z-ring grows smaller during septal ingrowth remains open.

There is an energy barrier for the initiation and early steps of tubulin polymerization, providing a barrier to nucleation of new filaments (172). If this was true for FtsZ polymerization, it could provide a point for regulating protofilament formation during assembly of the Z-ring or the FtsZ spiral structures. It also is not known whether assembly or disassembly of FtsZ polymers within intact cells is modified by auxiliary proteins, as is true for microtubules in eukaryotic cells.

**(v) Regulation of Z-ring assembly and stability.** The assembly, stability, and function of the Z-ring and cytokinetic ring must be regulated both spatially and temporally during the normal division cycle. Spatial regulation restricts Z-ring formation to the desired site for later septum formation (reviewed in reference 175). This is accomplished primarily by the Min site selection proteins, which are organized into a cytoskeletal system that is discussed later in this review. Temporal regulation is required to ensure that septum formation occurs at the correct time in the cell cycle, after chromosome replication and segregation are completed. Control of cellular FtsZ protein concentration by regulation of transcription, translation, and/or degradation may play a role in regulating Z-ring formation in some cases, as, for example, during the cell cycle of *C. crescentus* (97, 165, 179). However, in most cases regulation is accomplished by the use of positive or negative effector proteins that regulate Z-ring assembly or stability. A number of effector proteins have been identified (Table 1) (reviewed in references 133 and 172), and others probably remain to be discovered. Thus far it is not known how these or other regulatory factors determine the timing of septation in the cell.

Regulation of Z-ring formation is also used as a damage control mechanism in cases of delayed chromosome segregation or of DNA damage (212, 221). In these cases, irreparable DNA damage would result if septation took place over unsegregated chromosomes or before damaged DNA is repaired

and segregated by the cell. To prevent this, Z-ring formation is blocked as part of the SOS response to DNA perturbations until the defect is corrected (221).

**BtubA/B.** A second group of bacterial tubulin homologs is exemplified by the BtubA and BtubB (bacterial tubulin) proteins. Unlike FtsZ, which is present in almost all bacterial species, BtubA and BtubB have thus far only been identified in the genus *Prostheco bacter* in the division *Verrucomicrobia*. The proteins from *Prostheco bacter de j on ge ii* have been studied in some detail. BtubA and BtubB are the only tubulin homologs in this organism, and electron crystallographic studies indicate that the three-dimensional structures of the BtubA monomer and BtubA/B heterodimer resemble those of tubulin (Fig. 1B) (183). Several lines of evidence, including similarities in polymerization properties, suggest that the BtubA/B system may provide a good model system for studying certain aspects of tubulin behavior and microtubule assembly.

**(i) BtubA/B polymerization.** BtubA and BtubB copolymerize in the presence of GTP into double-helical protofilaments and small rings (183, 192). Filament formation requires both proteins, although BtubB can self-assemble into ~35-nm-wide rings in the absence of BtubA, whereas BtubA cannot polymerize by itself. The BtubA/B protofilaments self-associate into bundles that are sometimes organized around a central cavity, generating a microtubule-like structure. The distance between helical turns of the BtubA/B protofilament is similar to that of tubulin and FtsZ protofilaments (183). The cooperative mode of polymerization and the self-assembly of the polymers into tubular structures (192) are reminiscent of the assembly of microtubular structures from eukaryotic tubulin, which also are composed of heterodimer subunits ( $\alpha\beta$ -tubulins). BtubA/B polymerization is also associated with an increase in GTPase activity, similar to the polymerization-dependent GTPase activation that occurs with both tubulin and FtsZ polymerization. The BtubA/B tubular structures are thicker than eukaryotic microtubules (~40-nm versus 25-nm outside diameters) and are composed of two layers of protofilaments instead of a single layer. Stable polymers were also formed when BtubA and BtubB were coexpressed in *E. coli* cells, as shown by the formation of long, straight filaments that reacted with anti-BtubB antibody (192). Similar localization studies have not yet been done in *P. de j on ge ii* to confirm the likely supposition that the intracellular tubular structures are composed of BtubA/B. Since *P. de j on ge ii* does not contain an equivalent of the tubulin homolog FtsZ in the 95% of the genome that has been completed, it is conceivable that BtubA/B might also play a role in cytokinesis.

**Microtubule-like structures in *Verrucomicrobia*.** Ectosymbionts of marine hypotrich ciliates (*Euplotidium* species) have been characterized as *Verrucomicrobia*, the division that also includes *P. de j on ge ii* (see above), although they are distinct from *P. de j on ge ii* (158). During one stage of its complex life cycle, the ectosymbiont develops an extrusive apparatus designed to protect against predators. The apparatus is surrounded by a basket consisting of bundles of tubular structures which remain within the cell after the apparatus is extruded. The outside diameter of the tubules is ~22 nm, and the diameter of the lumen is ~13 nm (cited in reference 158), similar to the dimensions of eukaryotic microtubules (206). The tubules react with several monoclonal antitubulin antibodies and dis-

assemble in the presence of the microtubule inhibitor nocodazole, supporting the idea that they are counterparts of eukaryotic microtubules (158, 173). The constituents of these tubular structures have not yet been identified, and it is not yet known whether the organisms contain Btub homologs.

The fact that microtubular structures are present in these organisms and the demonstration that the BtubA/B proteins of *P. de j on ge ii* resemble  $\alpha\beta$ -tubulins in their ability to polymerize into tubular structures suggest that the verrucomicrobial systems may prove useful for the study of aspects of tubulin and microtubule behavior, especially if appropriate genetic systems can be developed.

### Intermediate Filament Protein Homologs

Intermediate filament proteins comprise the third major class of eukaryotic cytoskeletal protein. Until the identification of the bacterial IF-like protein crescentin, IF proteins were believed to be unique to animal cells (25). The major role of intermediate filaments is to act as a skeletal scaffold that helps maintain cell shape and cellular and nuclear integrity by protecting against mechanical stresses (reviewed in references 71, 72, and 104). There are a number of eukaryotic IF protein subclasses, based on sequence analysis and cellular distribution. These include cytoplasmic IF proteins (keratins, vimentin and desmin, and neurofilament triplet proteins) and nuclear lamins (71, 72, 104). The association of intermediate filaments with microtubules is required for the maintenance of the IF network (reviewed in reference 22).

**Crescentin.** Crescentin is the only cytoskeletal IF homolog thus far identified in prokaryotic cells. It is responsible for the shape of the comma-shaped organism *C. crescentus* (8) and was identified in a screen for *C. crescentus* transposon insertion mutations that affected cell shape. Loss of the structural gene for crescentin, *creS*, leads to a change in cell shape from comma to rod. The assignment of crescentin as an IF protein homolog is based primarily on its predicted protein domain organization. Crescentin has approximately 25% sequence identity and 40% similarity to eukaryotic IF proteins. However, it was pointed out that there are similar degrees of sequence similarity to non-IF proteins that contain extensive coiled-coil motifs (8). More specifically, crescentin and IF proteins share a predicted domain organization of four central coiled-coil structures with a characteristic discontinuity in the heptad repeat structure within the last coiled-coil segment (72).

Evidence that crescentin forms a cytoskeletal structure within the cell came from immunofluorescence studies showing that crescentin is present as an extended filamentous structure along the concave side of the *C. crescentus* cell (Fig. 4C) (8). This was confirmed in living cells by study of nonfunctional crescentin-GFP fusions which were coexpressed with untagged crescentin and by the observation that the curved shape of the cell is lost when crescentin is absent (8). These results suggest that the filamentous structure along the inner curve of the cell is a crescentin-based cytoskeletal element that establishes or maintains the comma shape of the cell.

The presumption that the curved cellular filamentous structures are composed of crescentin is supported by in vitro studies showing that purified crescentin rapidly self-assembles into long filaments. The self-assembly process does not require

nucleotides or other cofactors, thereby resembling IF protein polymerization and differing from the polymerization of bacterial or eukaryotic tubulin or actin homologs (8). The crescentin filaments also resemble eukaryotic IFs in their fast assembly and viscoelastic properties, indicating that the crescentin network is solid-like and resistant to mechanical strains (Osigwe Esue and Denis Wirtz, personal communication). However, crescentin filaments differ from eukaryotic IFs in their poor mechanical resilience and absence of strain stiffening after mechanical shearing.

Interestingly, crescentin and MreB cytoskeletal structures are both required for production of a comma-shaped cell. In the absence of MreB, *C. crescentus* cells become spherical despite the presence of crescentin, whereas loss of crescentin in the continuing presence of MreB leads to a comma-to-rod transition (8). This implies that MreB is required for the longitudinal mode of cell growth that leads to a rod shape, whereas the role of crescentin is to impart a curvature to the rod-shaped cell. The curved shape is not intrinsic to the crescentin polymeric structure, since crescentin polymerizes in vitro into linear filaments. The fact that isolated murein sacculi of *C. crescentus* retain their general curved shape (163) also argues against the idea that a rigid crescentin skeletal structure plays a mechanical role in shape determination. Thus, it appears that crescentin acts indirectly in establishment of the comma shape by directly or indirectly affecting the cellular organization of the shape-determining murein biosynthetic machinery. MreB is normally required for organization of the murein biosynthetic components into a longitudinal helical arrangement (discussed above). Because crescentin alters cell shape only in cells that also contain MreB, crescentin may act by imparting a curved shape to the otherwise longitudinal helical organization of the MreB cytoskeleton, thereby secondarily altering the cellular distribution of the murein biosynthetic machinery.

### The MinD/ParA Class of Bacterial Cytoskeletal Proteins

In addition to homologs of eukaryotic cytoskeletal proteins, bacterial cells contain another group of cytoskeletal proteins that have no homology to eukaryotic cytoskeletal elements. These belong to the large MinD/ParA superfamily. They are characterized by the presence of deviant Walker A-type ATPase motifs (102, 222) and are classified as cytoskeletal proteins on the basis of their presence in organized filamentous structures within cells and, where examined, their ability to self-assemble into long polymeric filaments in vitro. The use of Walker-type ATPase proteins as cytoskeletal components appears to be unique to bacterial cells. They are distinguished from the large group of noncytoskeletal Walker type ATPases by the presence of a deviant Walker A motif (GXGGXHK[TS]) within the nucleotide-binding P-loop that is located near the N termini of the proteins (102), although a few noncytoskeletal bacterial proteins also contain the deviant Walker A motif, including NifA, ArsA, and others (102, 222).

We divide the MinD/ParA proteins into two subgroups. Proteins of the MinD subgroup are involved in placement of bacterial and plastid division sites, whereas proteins of the ParA subgroup are involved primarily in DNA partition. MinD

homologs in eubacteria and plastids have a highly conserved six-amino-acid sequence called the MinD box (GLRNLD) which is not present in proteins of the ParA subgroup (224).

**Subgroup 1: MinD. (i) The MinCDE system.** MinD is a cytoskeletal protein that plays a key role in determining the site of septal placement in *E. coli*, in cooperation with the other two gene products of the *min* operon, MinC and MinE (reviewed in reference 175). Min proteins also regulate division site placement in other prokaryotic species and placement of the organellar division sites of plastids of plants and photosynthetic bacteria (5). The Min proteins restrict septation to the desired midcell site by preventing assembly of the division machinery at sites nearer the ends of the cell. In *E. coli* this involves a unique oscillation cycle in which the proteins become concentrated within a membrane-associated polar zone that oscillates from pole to pole. As discussed below, the pole-to-pole oscillation of the Min proteins involves the cyclical redistribution of the proteins within a MinD cytoskeletal framework that extends along the length of the cell (187). In *B. subtilis*, which lacks a MinE homolog, nonoscillating MinCD polar zones are present at both ends of the cell (135, 136). Formation of the *B. subtilis* polar zones is regulated by the DivIVA protein, which is unrelated to MinE and appears to utilize a different localization mechanism (42, 43). Some bacteria, such as *C. crescentus*, lack Min protein homologs, and it is not known how division site selection is carried out in these organisms. The cytoskeletal organization of the Min proteins has thus far been reported for the *E. coli* (187) and *Neisseria gonorrhoeae* (201) proteins.

**(ii) The MinD cytoskeleton.** High-resolution fluorescence microscopy using optical sectioning and deconvolution techniques have shown that MinD molecules, together with MinC and MinE, are organized into helical structures that coil around the *E. coli* cell cylinder just inside the cytoplasmic membrane (Fig. 6A to D) (187). In some cases the structures appear to be composed of a pair of intertwined helical strands. Although the MinD helical structures resemble the coiled structures that comprise the MreB cytoskeleton (compare Fig. 2A and 6B), the MreB and MinD helical arrays are independent structures as shown by their different helical densities (188) and by the differences between localization of the MreB and MinD coiled structures during the cell cycle. Although it is likely that each helical strand is composed of several MinD polymers, it is not known whether each strand consists of MinD polymers that extend from the cell pole to the end of the helical structures, as indicated in Fig. 6H, or whether each helical strand is composed of an array of shorter polymers.

In the original studies describing the helical organization of the Min system, the coiled MinD structures were clearly seen only in cells expressing MinD and MinE or expressing all three Min proteins. This suggested that MinE might be needed for organization or stability of the helical arrays. Since then, however, MinD helical structures extending between the two ends of the cell have been visualized in the absence of MinE or MinC (L. Ma and L. Rothfield, unpublished observations). Consistent with the conclusion that MinD is the basic structural element of the Min cytoskeletal structures, MinC and MinE are present in these structures only when MinD is also present (187).

In the absence of MinE, the coiled MinD or MinD/MinC

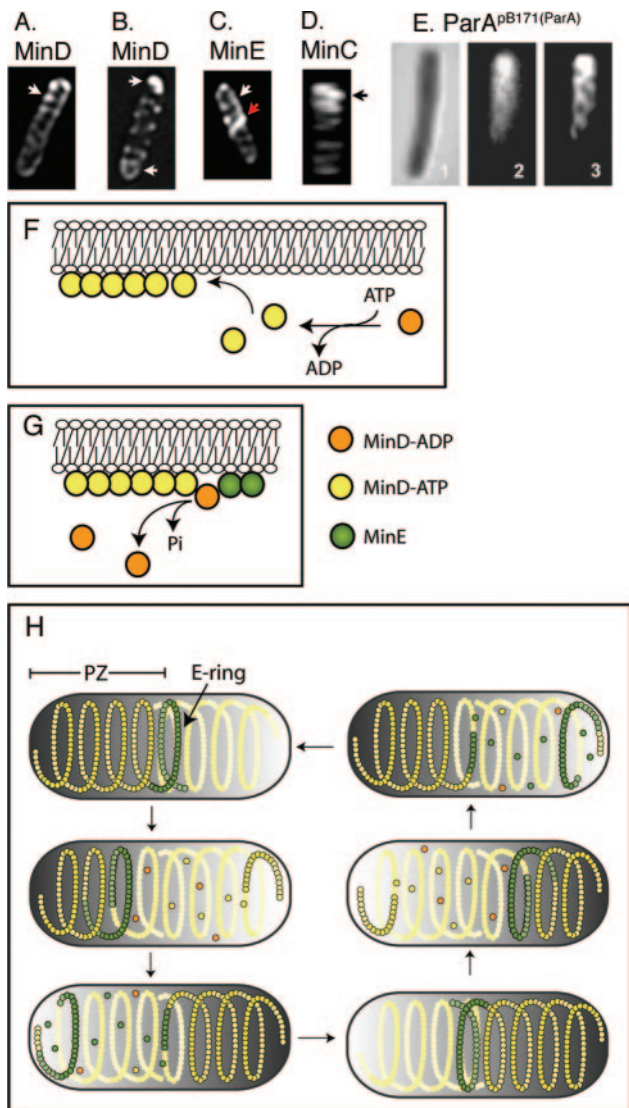


FIG. 6. Helical organization of the MinD/ParA cytoskeletal proteins. (A to D) Fluorescently labeled MinD (A and B), MinE (C), and MinC (D). (Reprinted from reference 187 with permission of the publisher. Copyright 2003 National Academy of Sciences, U.S.A.) (A and B) Helical distribution of MinD when coexpressed with MinE. (A) A bright MinD helical structure is present at one end of the cell, representing a MinD polar zone (white arrow). A less intense coiled structure extends to the other end of the cell, presumably representing the underlying pole-to-pole MinD helical structure. (B) Short MinD polar zones are visible at both ends of the cell (white arrows), one presumably representing a growing zone and the other representing a polar zone at the opposite end of the cell, in the last stage of disassembly, as depicted in panel H. (C) Helical distribution of MinE when coexpressed with MinD. The majority of the MinE molecules are present in an end loop (the MinE ring, red arrow) of the MinE helical array that represents the polar zone. The white arrow indicates polar zone coils. Micrographs in panels A to C are deconvolved images. (D) Helical distribution of MinC when coexpressed with MinD and MinE (three-dimensional reconstruction from an optically sectioned cell). The arrow indicates the MinC coils of the polar zone. (E) Helical distribution of fluorescently labeled ParA from plasmid pB171. 1, Nomarski image; 2, raw image; 3, deconvolved image. (Reprinted from reference 39 with permission from Blackwell Publishing.) (F) Mechanism of MinD polymer growth on the cytoplasmic face of the inner membrane by addition of MinD-ATP subunits. (G) Stimulation of disassembly of MinD-ATP polymer by a MinE ring. MinE molecules

structure appears to extend between the two ends of the cell. However, MinE provokes the dramatic redistribution of most of the MinD, MinE, and MinC molecules to the helical coils at one end of the cell (the polar zone) (Fig. 6A to D) (187). In addition to its presence in the polar zone, in many cells MinE is also present in a second structure, the MinE ring. The MinE ring represents an extension of the polar MinCDE helical structure, within which a high concentration of MinE gives the appearance of a ring (Fig. 6C). The polar zones and E-rings undergo repetitive pole-to-pole oscillations in which the structures are repetitively assembled and disassembled at alternate poles with a period of  $\sim 90$  s per cycle (78, 167, 168, 177), as discussed further below.

**(iii) MinD structure.** The crystal structures of MinD from three thermophilic organisms have been determined, i.e., MinD-1 of *Archaeoglobus fulgidus* (24) (Fig. 1C), MinD of *Pyrococcus furiosus* (68), and MinD-2 of *Pyrococcus horikoshii* (180). The three proteins are similar in primary sequence and three-dimensional structure. The proteins were crystallized as the ADP-bound form (68, 180), as MinD bound to the ATP analog AMPPCP (68), and as the nucleotide-free protein (24). In all cases MinD was present as a monomer. Gel filtration studies have suggested that MinD at relatively high concentrations can dimerize in the presence of ATP (76), and it has been proposed that ATP-induced dimerization plays a role in the membrane association of MinD (76, 77). The failure to observe dimers in the X-ray studies may reflect the failure to thus far crystallize the native ATP-bound form of the protein.

The structures of MinD from the thermophilic species have been extensively used to guide structure-function studies of *E. coli* and other organisms (77, 128, 201). However, there have not yet been any studies of biological function or cellular organization of MinD in the thermophilic organisms. In addition, the thermophilic strains lack apparent MinC and MinE counterparts. Thus, it is not known how functionally similar the thermophilic MinD proteins are to the MinD proteins of *E. coli*, *B. subtilis*, and *N. gonorrhoeae*, for which most cell biological studies have been done but whose three-dimensional structures have not yet been determined.

**(iv) MinD polymerization.** MinD polymerizes into short double-stranded filaments when incubated with ATP, with a filament width sufficient to accommodate one linear MinD polymer in each strand (198). Strikingly, the addition of bilayer-bounded phospholipid vesicles causes the MinD filaments to increase greatly in number and length and to self-associate into filament bundles, consistent with the idea that the protofilaments of the MinD helical cytoskeleton self-assemble on the

in the E-ring stimulate the ATPase activity of the terminal MinD-ATP subunit in the polymer. Hydrolysis converts MinD-ATP to MinD-ADP, which is released from the end of the polymer. (H) Cyclic assembly and disassembly of the MinD helical polar zones (PZ) and MinE ring, leading to pole-to-pole oscillations. MinD-ATP subunits are yellow, MinD-ADP subunits are orange, and MinE subunits are green. See text for details. The solid yellow helical structures represent the underlying MinD helical structure that extends between the two ends of the cell. MinD helical structures also contain MinE and MinC, which are not shown for simplification.

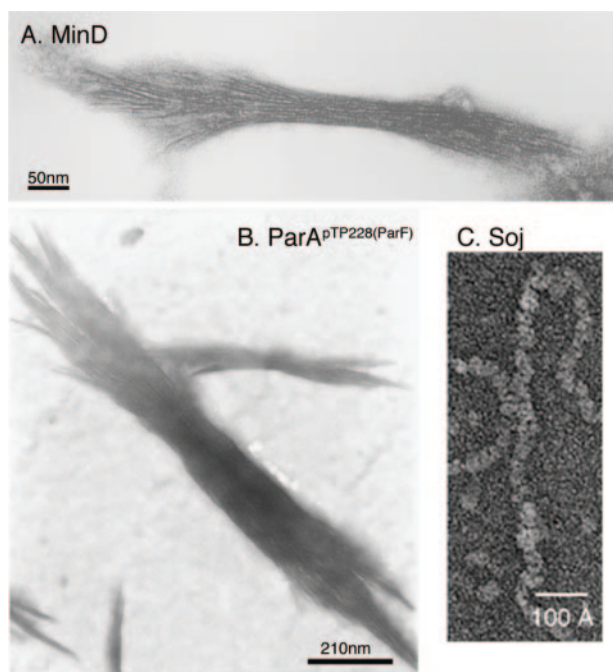


FIG. 7. In vitro polymerization of cytoskeletal proteins of the MinD/ParA superfamily. (A) Formation of MinD filament bundles in the presence of MinE, ATP, and phospholipid vesicles. One end of the bundle is markedly frayed because of the presence of MinE. (Reprinted from reference 198 with permission of the publisher. Copyright 2003 National Academy of Sciences, U.S.A.) (B) Formation of a ParA<sup>TP228</sup>(ParF) filament bundle in the presence of ParB<sup>TP228</sup>(ParG) and ATP. ParB<sup>TP228</sup>(ParG) stimulates formation of the frayed end(s) of the ParA<sup>TP228</sup>(ParF) bundle. (Reprinted from reference 11 by permission from Macmillan Publishers Ltd.) (C) Formation of Soj filaments in the presence of DNA and ATP. (Reprinted from reference 116 by permission from Macmillan Publishers Ltd.)

surface of the cytoplasmic membrane.

Addition of MinE significantly increases the extent of bundling (Fig. 7A) (198). This implies increased side-by-side interactions of the MinD protofilaments, due either to MinE cross-linking or to MinE-induced conformational changes. MinE exists as an antiparallel dimer, with the N-terminal domain of each of the two subunits extending from opposite sides of the dimer structure (100). Since the N-terminal domain contains the MinE sites which interact with MinD (127), this provides a plausible mechanism whereby MinE dimers can cross-link adjacent MinD filaments to form the MinD bundles (198). The ability of MinE to induce bundling of MinD filaments could explain the increase in protofilament number that is implied by the high concentration of MinD and MinE within the helical coils of the polar zones (Fig. 6A and C).

Paradoxically, MinE also causes disassembly of the MinD filaments in a process that involves activation of the MinD ATPase activity (79, 198). This may be related to the observation that the thick MinD bundles that form in the presence of MinE and phospholipid show marked fraying, predominantly at one end of the filament bundle (198) (Fig. 7A). This implies that in addition to interacting along the length of the filaments to promote bundling, MinE may also bind to one end of the filament bundle. This may explain the fact that the MinE ring

is formed at only one end (the medial end) of the helical structure that comprises the MinDE polar zone (Fig. 6C and H). The fraying could represent a stage in the filament disassembly reaction that is induced by MinE in vitro (198) and by the MinE ring in vivo (186). Similar fraying occurs at one end (the plus end) of microtubule bundles during microtubule disassembly (7). It is not known whether the MinD bundling and fraying effects can be dissociated by varying the MinE concentration.

**(v) Membrane targeting of MinD.** The membrane association of MinD is mediated by a C-terminal membrane-targeting sequence (MTS) that varies between 8 and 12 amino acids in different species (77, 202). The isolated MTS is unstructured in an aqueous environment but is converted to an amphipathic  $\alpha$ -helix when it interacts with phospholipid bilayers (203). The C-terminal region that comprises the MTS of the *A. fulgidus* MinD (determined in the absence of phospholipid) is also unstructured (24). The hydrophobic side chains of the amino acids on the nonpolar face of the amphipathic helix intercalate into the bilayer, thereby anchoring the protein to the membrane (203, 226). The membrane association is then stabilized by polymerization of the membrane-bound MinD (203).

MinD molecules from many species contain a similar MTS, and a similar MTS also mediates the membrane attachment of the *E. coli* cell division protein FtsA (159). The MTS sequences of FtsA and MinD can be interchanged without significant effect on membrane binding or protein function (159). Although all MinD MTSs are predicted to have a high propensity to form amphipathic helices, there are differences in sequence and in the length of the helices that can lead to differences in affinity for different lipids and in strength of membrane binding (203). This may provide a mechanism to optimize the protein for use in organisms with different membrane phospholipid compositions (203).

The MinD MTS can be replaced by the totally unrelated hydrophobic 43-amino-acid membrane anchor of cytochrome *b*<sub>5</sub> without interfering with its targeting to the *E. coli* membrane and formation of the membrane-associated helical cytoskeletal structures (204). However, MinD containing the cytochrome *b*<sub>5</sub> membrane anchor loses the ability to form polar zones in *E. coli* cells in the presence of MinE (204). This may indicate that the large hydrophobic cytochrome *b*<sub>5</sub> membrane-binding domain may prevent redistribution of the membrane-associated MinD by increasing the strength of its membrane association.

Some putative MinD homologs do not contain a recognizable MTS. The significance of this is unknown, since biological or biochemical studies of MinD function have been carried out only with a few species.

**(vi) MinD-bilayer interactions.** MinD is the first well-studied example of a bacterial cytoskeletal element that binds directly to membranes. MinD binds to phospholipid vesicles in the presence of ATP or a suitable nonhydrolyzable ATP analog, but not in their absence (76, 110). Therefore, nucleotide binding is sufficient to support the membrane binding of MinD. It has been suggested that the role of ATP binding is to promote the formation of MinD dimers in the cytoplasm, leading to a conformational change that exposes the membrane-binding sequences (126). Consistent with this model, ATP induces formation of MinD dimers in the absence of phospholipid,

although at relatively high concentrations of MinD (77). Alternatively, rather than acting by promoting MinD dimerization, ATP binding may induce a conformational change that exposes or activates the membrane-targeting domain, with oligomerization occurring after membrane association (202, 204). Consistent with this idea, loss of membrane binding due to removal of the MinD MTS leads to a 25-fold reduction in MinD-MinD interaction in yeast two-hybrid assays (204).

Strikingly, the ATP-dependent interaction of MinD with phospholipid vesicles leads both to MinD polymerization and to vesicle deformation, with the formation of long lipid tubes approximately 50 to 100 nm in diameter that extend from the vesicle surface (76). Tubulation was not reported in another study of MinD-vesicle interactions, where the MinD filaments were observed to often wrap around and deform the lipid vesicles (198). This difference presumably reflects differences in protein preparations or experimental conditions. The ATP analog ATP $\gamma$ S did not induce tubulation, although it did promote MinD binding to vesicles. The reason for this has not been clarified (76).

Addition of MinE reverses the tubulation reaction, presumably because of its ability to stimulate MinD polymer disassembly (discussed below). Tubulation of phospholipid vesicles is also induced by several eukaryotic proteins involved in vesicle formation and by dynamin (85, 200). It would be of considerable interest if a similar tubular deformation of the cytoplasmic membrane is associated with MinD polymerization in vivo. However, there is as yet no evidence that the tubulation phenomenon has any biological significance, and it may be restricted to the in vitro system. Nevertheless, it suggests that some type of perturbation of the membrane bilayer could play a role in MinD function within the cell.

**(vii) Dynamic rearrangements of the MinD cytoskeleton.** Pole-to-pole oscillation of the Min proteins is essential for their role in division site selection (175). The oscillations result from an ordered sequence of cytoskeletal rearrangements in which MinC, MinD, and MinE molecules are redistributed from polar coils at one end of the cell into the polar coils at the other end of the cell. During these events, the underlying helical structure that extends between the two ends of the cell appears to remain in place. The cytoskeletal rearrangements that lead to the pole-to-pole oscillatory behavior are believed to occur in the following way (Fig. 6F to H).

**(a) Polar zone assembly.** Membrane-associated MinD-ATP polymerizes in a helical pattern from the cell pole toward midcell, possibly using a preexisting MinD helical cytoskeleton that extends the length of the cell as a scaffold or template (Fig. 6A, F, and H). It is not known whether polymerization initiates at preexisting nucleation sites near the poles or occurs stochastically without specific nucleation sites. A mathematical model that includes polar nucleation sites reproduces all of the relevant characteristics of the oscillatory system, including the E-ring and polar zones (36). However, stable self-perpetuating oscillatory systems can also be generated in the absence of polar nucleation sites, as shown by other mathematical treatments that include neither polymers nor nucleation sites but are based only on the diffusion characteristics and assumed affinities of the proteins for each other and for the membrane (81, 98, 105, 138). During assembly of the polar zone, MinD recruits MinC and MinE, converting the helical MinD polar

zone to a MinDCE polar zone. Attachment of MinC and MinE may take place after MinD has polymerized on the membrane surface, although the primary interactions with MinD could also occur in the cytosol (204), with MinD-MinC and/or MinD-MinE complexes moving to the membrane concurrent with MinD polymer assembly.

**(b) MinE ring assembly.** When the growing ends of the MinD polymers approach midcell, addition of MinD-ATP slows and MinE assembles at the growing ends of the helical protofilaments to create a MinE-enriched extension of the coiled structures (the E-ring) (Fig. 6C and H). The ability of MinE to outcompete MinD probably reflects depletion of the cytoplasmic pool of MinD that occurs during growth of the polar zone (36). The E-ring is believed to play two roles. First, it blocks extension of the polar zone past midcell by acting as a cap to prevent further addition of MinD subunits. This was suggested by the observation that MinE mutations that prevent formation of the E-ring lead to growth of the polar zones well beyond their normal limit near midcell (186). Second, the E-ring activates the MinD ATPase activity at the leading edge of the MinD-ATP polymers (79).

**(c) Polar zone disassembly.** Activation of the MinD ATPase leads to conversion of MinD-ATP to MinD-ADP, which is released from the end of the MinD polymer because of its low affinity for the membrane (Fig. 6G). This results in progressive shortening of the coiled MinDCE polar structure until it disappears together with the E-ring (Fig. 6H). In vitro studies show that MinD-ADP is released from phospholipid vesicles into the aqueous medium when the MinD ATPase is activated by MinE (76, 110). If this accurately mimics the disassembly of the polar coiled structures in vivo, it would imply that disassembly is accompanied by release of the proteins into the cytoplasm, as suggested by fluorescence microscopy of labeled MinD in intact cells (168).

**(d) Oscillation.** The released MinD-ADP is converted to MinD-ATP and moves to the other pole to repeat the assembly-disassembly cycle, thereby continuing the oscillation cycle (Fig. 6F and H). The proteins may move to the opposite end of the cell by simple diffusion or by some undefined facilitated translocation mechanism. Based on the known diffusion rates of molecules within the *E. coli* cytoplasm (approximately  $2.5 \mu\text{m}^2 \text{ s}^{-1}$ ) (44), movement by simple cytoplasmic diffusion would be fast enough to account for the temporal characteristics of the oscillation process (36, 81). There is no evidence that the proteins are transported to the opposite pole by movement along the helical MinD structure or along another cytoskeleton-like structure, although this possibility has not been definitively excluded. The Min oscillatory system functions in the absence of MreB (188), eliminating the possibility that the MreB cytoskeleton participates in the end-to-end translocation of the Min proteins.

The energy to drive the oscillation cycle comes from the topological coupling of MinD-ATP hydrolysis to the assembly and disassembly of the helical filamentous structures. Cycles of polymer assembly and disassembly driven by nucleotide binding and hydrolysis also play a key role in the biological function of the ParM protein (discussed above).

**Subgroup 2: type I plasmid partitioning proteins.** Many systems responsible for the equipartition of low-copy-number plasmids into daughter cells use plasmid-encoded cytoskeletal

structures as part of the DNA segregation machinery. Type I partitioning systems are the most common of the plasmid partitioning systems and are defined by the presence of Walker-type ATPase proteins that are related to the MinD protein of the division site selection system (41, 69). Type II partitioning systems utilize actin homologs as the cytoskeletal ATPase component in the partitioning system. Occasionally the same plasmid contains both type I and type II partitioning systems, as in the case of *E. coli* and *Salmonella enterica* serovar Typhimurium plasmids pB171 and R27 (41). The type I and type II partitioning systems represent the two major mechanisms of ensuring stable inheritance of low-copy-number plasmids in bacterial cells. For a review of plasmid partitioning mechanisms, see references 41 and 69.

In this section we discuss the cytoskeletal aspects of type I plasmid partitioning systems. We also separately discuss the chromosomal Soj protein, which is a member of the same Walker-type ATPase family. Chromosomal ParA and ParB homologs that are required for faithful chromosome partition in several organisms have also been identified (4, 62, 99, 144), but there is as yet no evidence that these are present in cytoskeletal structures. Type II systems, exemplified by the ParM protein of plasmid R1, were discussed elsewhere in this review.

**(i) ParA/B proteins in plasmid partitioning.** All of the known type I partitioning systems consist of a *cis*-acting centromeric DNA site (variously named *parC* or *parS* and called *parC* [centromere] below in this review) and two plasmid-encoded proteins. The three components are normally encoded by partitioning loci (*par* loci) within the plasmid genome, although the protein components can function even when expressed in *trans* to the centromeric DNA (41, 154). The first protein is the Walker-type ATPase, variously named ParA, SopA, or Par F and called ParA below in this review [for example, ParA<sup>F(SopA)</sup>]. [In the terminology used for type I plasmid partition proteins, ParA and ParB represent the Walker-type ATPase protein and the centromere-binding protein, respectively. Superscripts indicate the plasmid name and, in parentheses, the common name of the protein in the specific plasmid. For example, ParB<sup>F(SopB)</sup> refers to the centromere-binding partition protein of plasmid F, which is commonly called SopB.] The ParA proteins are responsible for segregating the two daughter plasmids to opposite halves of the cell. The ParA proteins show sequence similarity to MinD and to each other, chiefly within the deviant Walker-type ATPase motifs. They lack the C-terminal membrane-targeting sequence that anchors MinD to the cytoplasmic membrane, and there is no evidence that the ParA proteins are membrane associated. ParA proteins also lack the MinD box that is characteristic of MinD proteins (224). The second protein, variously named ParB, SopB, or ParG, is a specific centromere-binding protein and is called ParB below in this review [for example, ParB<sup>F(SopB)</sup>]. ParB is required to provide a link between the plasmid and the ParA protein. It has been suggested that ParB may also be responsible for pairing of the two newly replicated plasmids to facilitate plasmid segregation as in the type II partitioning system (94, 154), although other models that do not require plasmid pairing have been suggested (41). Both ParA and ParB proteins may also play a role in transcriptional autoregulation of the *par* operon (41, 69).

**(ii) ParA cytoskeletal structures.** Although only a few systems have been studied in detail, there is increasing evidence that MinD and the ParA plasmid partitioning proteins share the ability to assemble into dynamic cytoskeleton-like structures within *E. coli* cells. At this time the evidence is too fragmentary to clearly define the mechanisms used by the ParA cytoskeletal structures to carry out plasmid partition, but a number of important clues are emerging. We will concentrate here on a few systems for which information is available and the results seem clearest.

The ParA proteins that have been shown to form cytoskeleton-like structures in vivo are exemplified by ParA<sup>F(SopA)</sup> (2) and ParA<sup>pB171(ParA)</sup> (39), which are present as extended helical patterns (Fig. 6E) whose general appearance resembles the MinD helical arrays (Fig. 6A to D). The coiled structures vary in distribution in different plasmids. For example, ParA<sup>F(SopA)</sup> helical structures appear to extend between the two poles (2), whereas the ParA<sup>pB171(ParA)</sup> helical arrays are localized over the nucleoid (39). It is not known what determines these differences. Although ParB can also be present in the coiled arrays [e.g., ParB<sup>F(SopB)</sup> (2)], ParB proteins are not an essential part of the cytoskeletal structures. Thus, the ParA<sup>F(SopA)</sup> (2) and ParA<sup>pB171(ParA)</sup> (39) helical patterns are present in cells that do not express ParB, and the presence of ParB<sup>F(SopB)</sup> in the coiled structures is dependent on the presence of the corresponding ParA protein (2).

**(iii) ParA polymerization.** ParA proteins [i.e., ParA<sup>F(SopA)</sup> (120) and ParA<sup>pTP228(ParF)</sup> (10, 11)] polymerize in vitro into filamentous structures that are likely to be equivalent to the protofilaments of the in vivo cytoskeletal structures. The ParA polymerization systems resemble the MinD system in several respects, with ParB acting as an auxiliary protein analogous to MinE. First, MinD polymerization and ParA<sup>F(SopA)</sup> and ParA<sup>pTP228(ParF)</sup> polymerization are greatly stimulated by ATP (11, 120). In the MinD and ParA<sup>pTP228(ParF)</sup> polymerization systems, ATP can be replaced by a nonhydrolyzable analog, indicating that it is ATP binding, rather than ATP hydrolysis, that is required for polymerization in both cases (11). Second, low concentrations of ParB<sup>pTP228(ParG)</sup> potentiate the formation of ParA polymers, as shown by a significant increase in filament length and formation of bundles of protofilaments with a single frayed end (Fig. 7B) (11). These resemble the MinD bundles formed in the presence of MinE (198) (Fig. 7A). Third, the ATPase activity of ParA<sup>pTP228(ParF)</sup> is stimulated and polymer accumulation is inhibited by high concentrations of ParB<sup>pTP228(ParG)</sup> (11), possibly due to an increase in the rate of disassembly. This resembles the effects of MinE on the stability of MinD polymers in the presence of phospholipid bilayers. The ATPase stimulation is augmented in the presence of nonspecific DNA (11), raising the possibility that DNA may provide a suitable platform for the ParA<sup>pTP228(ParF)</sup> polymerization system in vitro and perhaps also in vivo, analogous to the role of phospholipid bilayers in the MinD system.

**(iv) ParA oscillation.** The similarity in behavior of the MinD and ParA proteins extends to the fact that some ParA proteins also show oscillatory behavior, with movement of foci between two positions within the cell. It should be noted that the ParA oscillatory systems have been less extensively studied than their Min counterpart, and the back-and-forth movement of the protein that comprises a complete cycle has not always been de-

scribed, nor have the movements in most cases been followed for more than one cycle to confirm their repetitive nature. Oscillation has been observed between the cell quarters [ $\text{ParA}^{\text{F(SopA)}}(120)$ ], between the cell poles [ $\text{ParA}^{\text{F(SopA)}}(120)$ ] (quoted in reference 2)], and over the nucleoid region [ $\text{ParA}^{\text{pB171(ParA)}}(39, 40)$ ]. In at least one case [ $\text{ParA}^{\text{pB171(ParA)}}(39, 40)$ ], it is clear that the oscillation reflects redistribution of the proteins within the coils of the ParA helical array (39), thereby also mimicking the Min oscillatory system (Fig. 6). The oscillation periods of  $\text{ParA}^{\text{pB171(ParA)}}$  and  $\text{ParA}^{\text{F(SopA)}}$  are approximately 20 min (40, 120), significantly slower than the reported MinD oscillation rates (168). However, the oscillation rate of MinD is significantly affected by the MinD/MinE ratio (168). The possibility that variations in ParA/ParB ratios could similarly affect the ParA oscillation rate has not yet been systematically examined.

Interestingly, although  $\text{ParA}^{\text{pB171(ParA)}}$  formed helical structures in the absence of ParB, oscillation required the presence of both  $\text{ParB}^{\text{pB171(ParB)}}$  and  $\text{parC}^{\text{pB171(parC)}}$  DNA (39). This is reminiscent of MinD oscillation, which also requires an accessory protein, MinE. It is likely that the ParA cytoskeletal structures play an important role in moving the daughter plasmids to their final positions in the two halves of the cell. This is implied by the observation that  $\text{ParA}^{\text{F(SopA)}}$  appears to shuttle between ParB foci (presumably representing ParB bound to plasmid *parC* sequences) that are located near the cell quarters (120). Additionally, a  $\text{ParA}^{\text{F(SopA)}}$  mutation that prevented ParA oscillations but did not prevent formation of intracellular ParA filamentous structures resulted in a defect in plasmid partition, implying a possible connection between the oscillation process and normal plasmid partition (120).

It is unclear how the cytoskeletal structures or the oscillatory behavior of the Par proteins mediates the plasmid translocation events. No single model is consistent with all of the present information. The following possibilities can be considered. (i) The ParA helical structure could function as a highway, with the ParB-plasmid complex acting as a cargo that is actively translocated to the ends of the ParA helical filaments in each half of the cell. (ii) The type I partition systems may resemble the *E. coli* Min system, with rapid pole-to-pole oscillation generating a concentration gradient in which the time-averaged concentration of a component (for example, the plasmid centromere-binding ParB protein) is high at two locations, one at each end of a normal length cell. This has been modeled mathematically for F plasmid partition in a complex model that includes other characteristics of the  $\text{ParA}^{\text{F(SopA)}}$ / $\text{ParB}^{\text{F(SopB)}}$  partition system and is based on a reaction-diffusion mechanism similar to that used in analyses of the Min oscillatory system (2). However, the ParA oscillations are quite slow compared to the Min oscillatory system (15 to 20 min versus 1 to 2 min), and a mechanism may be needed to keep ParB, and hence the ParB-plasmid complex, from diffusing away from its initial localization site between cycles. Another mathematical model includes ParA-nucleoid interaction and ParB-induced ParA polymer degradation and leads to oscillatory ParA waves although not to plasmid segregation (84). (iii) The type I partition systems may utilize a mechanism similar to the ParM system of plasmid R1 (discussed above). Growth or shrinkage of a ParA polymeric cytoskeletal array would push or pull the daughter plasmids to their final positions in the two halves of the cell. In this regard, it has been observed that incubation of

$\text{ParA}^{\text{F(SopA)}}$  together with the corresponding ParB protein and  $\text{parC}^{\text{F(sopC)}}$ -containing DNA led to formation of radial thin projections (asters) extending from a central core that included *parC* DNA and ParB protein (120). It was suggested that two similar structures, anchored to the two poles by the aster fibers, could be assembled on the progeny plasmids at midcell.  $\text{ParA}^{\text{F(SopA)}}$  polymerization between the two structures would push the plasmids to the two ends of the cell. In this mitotic spindle-like model, plasmid separation could also occur by shortening of the putative polar aster fibers. Neither the asters nor the polar  $\text{ParA}^{\text{F(SopA)}}$  fibers have yet been visualized within cells, and it will be of interest to see whether they are present in vivo.

The role of the ParA oscillatory behavior is obscure in all of the models discussed above except the second model. The possibility that different ParA-mediated partition mechanisms are used by different plasmids cannot be excluded, since a very limited number of systems have been studied. However, in view of the rapid accumulation of new data in this area, it is likely that the unanswered questions about these DNA partition systems will be clarified in the near future.

**Soj.** The Soj protein of *B. subtilis* is a member of the MinD/ParA family that performs several functions in concert with the Spo0J protein (62, 86, 121, 224). Spo0J recognizes centromere-like DNA sequences (*parS*) near the *B. subtilis* chromosomal replication origin (121), thereby resembling the plasmid-encoded ParB proteins which recognize plasmid centromeric loci. When the *parS* sequences are incorporated into low-copy plasmids, Spo0J and Soj function as a plasmid partition system that leads to faithful plasmid segregation into daughter cells (121, 224). In this process Soj acts as the ParA protein and Spo0J as the ParB equivalent.

Spo0J, but not Soj, is required for normal nucleoid segregation and for the oriented segregation of the chromosomal *oriC* region into the forespore during sporulation in otherwise normal cells (223). Soj and Spo0J also regulate expression of several genes during early stages of sporulation, with Soj acting as a transcriptional repressor that can be counteracted by Spo0J (21, 86). Soj has significant structural similarity to MinD, the only other ParA homolog whose three-dimensional structure is known (Fig. 1C) (116).

The normal biological role of Soj is not clear, although the plasmid partition experiments make it clear that it has the potential to function in DNA partition processes. Despite this, loss of Soj does not have obvious effects on nucleoid segregation. However, the possibility that Soj may have some role in chromosomal compaction, which is required for normal nucleoid partition, is suggested by the observation that loss of Soj in cells that lack the Smc chromosome compaction protein significantly increases the production of anucleate cells (114). Soj may also affect the segregation of the chromosomal origins (114). At this point the normal role of Soj in the life of the cell is still poorly defined.

The Soj-Spo0J interaction that is suggested by their cooperative roles in plasmid partition and sporulation is supported by the observation that the ATPase activity of Soj is markedly stimulated by Spo0J in the presence of nonspecific DNA (116). It has been pointed out that this is analogous to the stimulation of the ATPase activity of MinD by MinE in the presence of phospholipid bilayers (116). In this view, MinD and MinE play

roles similar to those of Soj and Spo0J, with the surface of the membrane bilayer playing a role in the MinD/MinE system that is equivalent to that of DNA in the Soj/Spo0J interaction (116, 180). Soj and MinD are also similar in their ability to dimerize in the presence of ATP (77, 116). It was suggested that Soj dimerization may create a site for binding of Spo0J in the presence of DNA (116). It was also suggested that a mechanism in which ATP-dependent dimerization leads to formation of a site for interaction with partner proteins (such as Spo0J and MinE) might be conserved among Soj, MinD, and ParA proteins, as well as some noncytoskeletal Walker-type ATPases, such as the nitrogen fixation protein NifH (116).

Soj resembles many cytoskeletal proteins in its ability to self-assemble into polymeric filaments in vitro in a reaction that requires ATP and nonspecific DNA (Fig. 7C) (116). Although there is no present evidence that Soj is present in cytoskeleton-like elements within cells, the ability of Soj to self-assemble in vitro into extended polymeric filaments, together with other properties that are similar to those of MinD and ParA proteins, raises the possibility that Soj may also be organized into filamentous cytoskeletal structures in intact cells, although these have not yet been detected.

Soj also resembles other members of the MinD/ParA family in undergoing repetitive changes in cellular localization in living cells, although the Soj oscillations differ significantly from the MinD and ParA patterns. Thus, GFP-labeled Soj localizes in patches over nucleoid regions and undergoes irregular Spo0J-dependent internucleoid and intranucleoid movements (134, 166), especially between nucleoids located near the two cell poles (9). Interestingly, the movements between nucleoids were partially dependent on the presence of MinD and also were suppressed by mutations that blocked cell division (9). The biological relevance of the dynamic behavior of Soj is unclear.

### Other Filamentous Intracellular Structures

Other filamentous intracellular structures in prokaryotic organisms have been described. In these cases the responsible proteins have frequently not been identified, and formation of polymeric filaments in vitro has usually not been demonstrated. These systems have not been studied to the extent of those described above. The following are examples of these structures.

***Spiroplasma melliferum* fibrillar structures.** Arrays of longitudinally oriented fibrillar structures have been observed by electron microscopy of intact and disrupted cells of *S. melliferum* (208–210). The structures contain a 55- to 59-kDa protein that has not been further identified. Electron cryotomography (109) visualized two types of filaments located beneath the cytoplasmic membrane in these cells. The filaments are arranged in three parallel ribbons extending along the length of the spiral-shaped organism. It was speculated that one of the filamentous structures may consist of the 55- to 59-kDa protein and the other of MreB (109). It has been suggested that these extended structures are responsible for the movement of the helical-shaped bacterium (109, 209).

***Treponema phagogenis* cytoplasmic filaments.** *T. phagogenis* cells contain arrays of approximately five parallel filamentous structures that curve along the length of the spiral-shaped cell,

dependent on expression of the *cfpA* gene (89). Although this distribution somewhat resembles the distribution pattern of crescentin in comma-shaped cells (discussed above), CfpA does not contain any predicted extended coiled-coil domains as found in crescentin and other IF-type proteins. Because of their locations relative to the periplasmic flagella of these organisms, a connection to cell motility has been suggested, although there is no evidence of a structural link between the flagella and the intracellular filamentous structures.

***Mycococcus xanthus* intracellular filaments.** Long bundles of submembranous filaments have been observed in *M. xanthus* cells (18). These may be related to a protein, AglZ, which has been implicated in regulation of gliding movement via the A-motility system of these organisms. The N-terminal region of AglZ resembles receiver domains of two-component response regulator proteins, whereas its C-terminal region includes heptad repeats characteristic of the rod region of coiled-coil proteins such as the myosin heavy chain (225). The latter domain self-assembles into filaments in vitro and forms ordered parallel arrays of filaments when expressed in *E. coli* (225). It is not known whether the intact protein forms similar structures in *Mycococcus* or other organisms.

***Mycoplasma pneumoniae* filamentous structures.** *M. pneumoniae* contains a complex rod-shaped intracellular structure that appears to represent an internal cytoskeleton (70). Similar structures have been observed in detergent extracts of intact *M. pneumoniae* cells (139, 170).

**Miscellaneous intracellular structures.** There are a number of examples where overproduction of a protein leads to the formation of intracellular filamentous structures. In these cases it is not clear whether these are polymerization artifacts due to the high concentration of the protein or whether they reflect an underlying propensity to form cytoskeleton-like structures. An example of this phenomenon is the formation of bundles of prominent axial filaments that extend along the length of the *E. coli* cell when the protein Rng (also called CafA) is overexpressed (219).

### HELICES, HELICES, AND MORE HELICES

Within the past 5 years, a number of cytoskeletal proteins have been shown to be present in extended helical structures within the cell, as discussed in this review. In addition to the cytoskeletal proteins, there are a growing number of other proteins that have been shown to assume helical cellular patterns. In these cases there is no evidence that the proteins can self-assemble into filamentous structures, and it seems unlikely that many of them will prove to be primary cytoskeletal elements within the cell. On the other hand, there is a good possibility that their helical distribution could result from secondary interactions with primary cytoskeletal elements. Most of these proteins are associated with the cytoplasmic membrane. They include the following examples.

#### SetB

SetB is an integral *E. coli* membrane protein that is present in helical structures along the length of the cell that resemble the MreB coiled cytoskeleton (49). SetB interacts with MreB in yeast two-hybrid experiments, suggesting that it may be asso-

ciated with the MreB cytoskeleton in the cell. The *setB* gene was identified as a multicopy suppressor of the chromosome partition defect resulting from a mutation in the *parC* gene that codes for a subunit of DNA topoisomerase IV (49). This and other observations suggest that SetB is involved in regulation of DNA conformation and/or segregation, although its exact function is not yet clear.

### Sec Proteins

The *B. subtilis* SecA and SecY proteins that are involved in protein translocation across the cytoplasmic membrane also assume a clustered distribution suggestive of a helical pattern (19). Similarly, the *E. coli* SecG and SecE proteins also appear to show a helical arrangement (190). This suggests that some or all of the components of the secretory machinery of the cytoplasmic membrane assume a similar organization, although the details remain to be firmly established.

### Tar

The aspartate chemoreceptor protein Tar is organized in helical patterns during its assembly into the membrane prior to its localization at the cell poles (190). These appear to reflect its association with elements of the secretory machinery, which also show a coiled distribution pattern (see above).

### Outer Membrane Components

Interestingly, several outer membrane components are also organized in a helical pattern along the long axis of the cell. Outer membrane components that show helical patterns include LamB, a transmembrane outer membrane protein which is distributed in highly mobile helical arrays (58); undefined proteins that can be labeled by nonspecific dyes from outside the cell (57); and lipopolysaccharide, which is located primarily in the outer leaflet of the outer membrane, identified by concanavalin A binding (57). In addition, five *C. crescentus* outer membrane proteins which were recovered from an MreC affinity column also showed clustering when their GFP-labeled derivatives were studied, which was interpreted as representing a spiral, punctate, or banding distribution pattern (35), as discussed earlier in this review.

In most of the examples cited above it is not known whether the proteins are associated with other cytoskeletal structures or whether they independently adopt a helical configuration within the cell. For outer membrane components, the coiled configuration could result from direct or indirect interactions with helical elements such as MreC, which are exposed in the periplasm (35), or by interaction with the murein sacculus, which may possibly be organized in a helical pattern (Fig. 2H).

### Why Is the Helical Distribution Pattern So Popular?

It is not clear why so many cytoskeletal proteins adopt a helical cellular configuration. This could simply reflect the fact that they are linear polymers composed of identical subunits, constrained to the inner surface of a cylinder such as the inner surface of the cytoplasmic membrane. In this case polymerization would always lead to a helical or coiled configuration

unless the contact sites between subunits were 180° apart on the surface of the protein (expressed relative to the long axis of the subunit) and the initial axis of polymerization was parallel or perpendicular to the long axis of the cylinder (see also reference 46). This could explain the relatively large number of apparently independent coiled structures in the cell. For structures such as the MreB cytoskeleton, which changes its helical organization and cellular distribution in growing cells, changes in the details of the subunit interactions and/or changes in interactions with specific cellular sites would be needed to explain the different arrangements that have been observed. Other mechanisms to explain the large number of helically organized proteins can also be imagined. These include a common, as yet unidentified, underlying helical scaffold structure within the cell envelope and use of the helical murein as a scaffold for inner or outer membrane proteins that have domains exposed to the periplasm. It is likely that different mechanisms will be responsible for the coiled configurations of different proteins.

## EUKARYOTIC AND PROKARYOTIC CYTOSKELETAL ELEMENTS

### Properties and Functional Relationships

Prokaryotic cells contain homologs for each of the three major groups of eukaryotic cytoskeletal proteins, i.e., actin, tubulin, and intermediate filament proteins, as discussed in this article. The three-dimensional structures of the eukaryotic and prokaryotic actin and tubulin homologs are generally quite similar despite relatively modest sequence homology in many cases. Eukaryotic and prokaryotic cytoskeletal proteins also share two important properties. First, they self-assemble into filamentous polymers *in vitro* in the presence of ATP (for most of the proteins) or GTP (for tubulin and tubulin homologs). Second, they are organized into ordered long-range structures within the cell.

In addition, eukaryotic and prokaryotic cytoskeletal elements participate in similar ranges of biological functions, including chromosome segregation, cytokinesis, regulation of cell shape, and establishment of cell polarity. Strikingly, however, the analogous function in prokaryotes and eukaryotes is not always carried out by cytoskeletal proteins from the same homology group. Thus, tubulin-based spindle fibers play a major role in eukaryotic chromosome segregation, whereas the similar function in prokaryotes is carried out by an actin homolog, such as MreB or the ParM protein of plasmid R1, or by representatives of the prokaryotic MinD/ParA group of cytoskeletal proteins which have no known eukaryotic equivalents. Similarly, actin forms the contractile ring that is required for cytokinesis in eukaryotic cells, whereas the tubulin homolog FtsZ is the key player in formation of the cytokinetic ring that constricts during septal invagination in bacterial cells. The differences between the functional roles of the eukaryotic and prokaryotic counterparts are accompanied in several cases by differences in polymerization properties. For example, eukaryotic tubulin polymerization *in vitro* leads to formation of tubular structures, whereas FtsZ polymerization does not lead to microtubular structures *in vitro* or *in vivo*. Additionally, tubulin polymers are characterized by dynamic instability associ-

ated with catastrophic filament disassembly events, requiring control by specific regulatory proteins in the cell. In contrast, dynamic instability has not been observed in polymerization of the bacterial tubulin homolog FtsZ but is characteristic of the bacterial actin homolog ParM.

In these examples there has been a role reversal both in polymerization dynamics and in biological functions. In many cases the important shared property of the prokaryotic and eukaryotic cytoskeletal homologs is limited to the ability to form polymeric filamentous structures, which in many cases show dynamic behavior that is regulated by nucleotide binding and hydrolysis. Beyond that, the organization of the filaments and their functional roles often differ considerably between eukaryotic and prokaryotic cells. These differences are presumably determined by differences in the structure of the protein homologs and in the properties of the host cells. A more careful analysis of the differences in protein structure between the bacterial and eukaryotic homologs, rather than concentrating on their similarities, seems warranted.

Eukaryotic cytoskeletal elements also perform important roles in intracellular transport or in force-generating events, in collaboration with motor proteins such as kinesin and dynamin (for microtubule-associated movement) or myosins (for movements along actin filaments) (4). Similar cytoskeleton-associated motor proteins have not yet been identified in prokaryotic cells. However, it is likely that they exist, and we anticipate that they will prove to play important roles in many of the translocation events discussed in this article.

### Membrane-Associated Cytoskeletal Structures

A number of cytoskeletal structures are associated with the membrane surfaces in both eukaryotic and prokaryotic cells (for example, the extensive actin-based or spectrin-based submembranous networks of most eukaryotic cells [4] and the MreB-, MinD-, and FtsZ-based cytoskeletal structures of bacterial cells). The filamentous cytoskeletal elements are anchored to the membrane in several ways. The primary filamentous cytoskeletal protein may directly interact with the lipid bilayer via a specialized membrane-binding domain such as the pleckstrin homology domain of spectrin (150) or the membrane-targeting sequence of MinD (77, 202). In other cases the membrane anchor is provided by cytoskeleton-associated proteins such as the ankyrin/band 3 membrane anchor of the spectrin submembranous cytoskeleton (4) or the suggested MreC membrane anchor of the *E. coli* MreB cytoskeleton (107). It is striking, and likely important, that the membrane anchors often have special affinity for specific lipids. For example, many eukaryotic cytoskeletal membrane anchors have high affinity for phosphoinositides (150), whereas MinD has a high affinity for acidic phospholipids (203). This could provide a mechanism to concentrate the initiation sites for polymerization or the cytoskeletal element itself in membrane regions enriched for the favored phospholipid, such as the poles of *E. coli* cells, which are enriched for cardiolipin (141).

One important role of the submembranous cytoskeletal networks of eukaryotic cells is to provide a framework for communication between the cell interior and the outside world via protein complexes that include transmembrane elements, such as the transmembrane integrin proteins that interact both with

extracellular matrix elements and with actin filaments in the periphery of the cell (4). In bacterial cells, the MreB/MreC/PBP transmembrane complex appears to play an analogous role by connecting the MreBC cytoskeleton to the murein layer of the cell envelope and regulating its biogenesis. Other systems of structural intracellular/extracellular communication systems in bacteria can be expected to emerge.

### CONCLUSIONS AND SUMMARY

The advances of the past 5 years have been extraordinary. Perhaps the most unexpected finding has been the large number of proteins that are organized into long-range ordered structures within the cell. However, with only a few exceptions, such as the ParM/ParF plasmid segregation system and the MinCDE division site selection system, we know practically nothing about how the cytoskeletal elements carry out such fundamental cellular functions as segregation of the chromosomes of the cell and most plasmids, constriction of the FtsZ ring, differentiation of the cell poles, or establishment of cell polarity, and we know only a bit more about the details of cell shape determination. In addition, the mechanisms underlying the surprising plasticity of some of the cytoskeletal structures are still poorly or not at all understood. This includes the remodeling of the MreB cytoskeleton during the cell cycle, the oscillatory behavior and other intracellular rearrangements of the ParA proteins, and the general reorganization of cytoskeletal elements that must occur during and after cell division. An understanding of these important and intriguing problems in bacterial cell biology will likely require, in many cases, a more complete identification of which proteins and protein complexes are associated with each of the primary cytoskeletal structures. Important information of this type is already emerging for the MreB/MreC/PBP, MinC/MinD/MinE, and FtsZ/septasome systems. It is likely, as in eukaryotic systems, that the integration of this information will reveal more complex cytoskeletal structures than are presently envisioned. Based on progress to date, we can be very optimistic about the advances to be expected during the next few years.

### ACKNOWLEDGMENTS

We acknowledge the help of Vitaliy Gorbatyuk in construction of protein three-dimensional figures, and we acknowledge Luyan Ma and Denis Wirtz for permission to quote unpublished information. We thank Mary Osborn for important help and advice and Stuart Austin, Miguel de Pedro, Jeff Errington, Kenn Gerdes, Giovanna Rosati, Christine Jacobs-Wagner, Dyche Mullins, Denis Wirtz, Andrew Wright, and other colleagues for helpful discussions.

Work from the laboratory of L.R. was supported by NIH grant GM R37-06032.

### REFERENCES

1. Abhayawardhane, Y., and G. C. Stewart. 1995. *Bacillus subtilis* possesses a second determinant with extensive sequence similarity to the *Escherichia coli* mreB morphogene. *J. Bacteriol.* 177:765–773.
2. Adachi, S., K. Hori, and S. Hiraga. 2006. Subcellular positioning of F plasmid mediated by dynamic localization of SopA and SopB. *J. Mol. Biol.* 356:850–863.
3. Addinall, S., E. Bi, and J. Lutkenhaus. 1996. FtsZ ring formation in *fts* mutants. *J. Bacteriol.* 178:3877–3884.
4. Alberts, B., A. Johnson, J. Lewis, M. Raff, K. Roberts, and P. Walter. 2002. *Molecular biology of the cell*, 4th ed. Garland Science, New York, N.Y.
5. Aldridge, C., J. Maple, and S. Moller. 2005. The molecular biology of plastid division in higher plants. *J. Exp. Bot.* 56:1061–1077.
6. Anderson, D. E., F. J. Gueiros-Filho, and H. P. Erickson. 2004. Assembly

- dynamics of FtsZ rings in *Bacillus subtilis* and *Escherichia coli* and effects of FtsZ-regulating proteins. *J. Bacteriol.* **186**:5775–5781.
7. Arnal, I., E. Karsenti, and A. A. Hyman. 2000. Structural transitions at microtubule ends correlate with their dynamic properties in *Xenopus* egg extracts. *J. Cell Biol.* **149**:767–774.
  8. Ausmees, N., J. R. Kuhn, and C. Jacobs-Wagner. 2003. The bacterial cytoskeleton: an intermediate filament-like function in cell shape. *Cell* **115**:705–713.
  9. Autret, S., and J. Errington. 2003. A role for division-site-selection protein MinD in regulation of internucleoid jumping of Soj (ParA) protein in *Bacillus subtilis*. *Mol. Microbiol.* **47**:159–169.
  10. Barilla, D., and F. Hayes. 2003. Architecture of the ParF-ParG protein complex involved in prokaryotic DNA segregation. *Mol. Microbiol.* **49**:487–499.
  11. Barilla, D., M. F. Rosenberg, U. Nobbmann, and F. Hayes. 2005. Bacterial DNA segregation dynamics mediated by the polymerizing protein ParF. *EMBO J.* **24**:1453–1464.
  12. Barna, J. C., and D. H. Williams. 1984. The structure and mode of action of glycopeptide antibiotics of the vancomycin group. *Annu. Rev. Microbiol.* **38**:339–357.
  13. Ben-Yehuda, S., and R. Losick. 2002. Asymmetric cell division in *B. subtilis* involves a spiral-like intermediate of the cytokinetic protein FtsZ. *Cell* **109**:257–266.
  14. Bernhardt, T. G., and P. A. de Boer. 2005. SlnA, a nucleoid-associated, FtsZ binding protein required for blocking septal ring assembly over chromosomes in *E. coli*. *Mol. Cell* **18**:555–564.
  15. Bi, E., and J. Lutkenhaus. 1991. FtsZ ring structure associated with division in *Escherichia coli*. *Nature* **354**:161–164.
  16. Bork, P., C. Sander, and A. Valencia. 1992. An ATPase domain common to prokaryotic cell cycle proteins, sugar kinases, actin, and hsp70 heat shock proteins. *Proc. Natl. Acad. Sci. USA* **89**:7290–7294.
  17. Bugg, T. D., S. Dutka-Malen, M. Arthur, P. Courvalin, and C. T. Walsh. 1991. Identification of vancomycin resistance protein VanA as a D-alanine: D-alanine ligase of altered substrate specificity. *Biochemistry* **30**:2017–2021.
  18. Burchard, A. C., R. P. Burchard, and J. A. Klotzel. 1977. Intracellular, periodic structures in the gliding bacterium *Myxococcus xanthus*. *J. Bacteriol.* **132**:666–672.
  19. Campo, N., H. Tjalsma, G. Buist, D. Stepniak, M. Meijer, M. Veenhuis, M. Westermann, J. P. Muller, S. Bron, J. Kok, O. P. Kuipers, and J. D. H. Jongbloed. 2004. Subcellular sites for bacterial protein export. *Mol. Microbiol.* **53**:1583–1599.
  20. Carballido-Lopez, R., and J. Errington. 2003. The bacterial cytoskeleton: in vivo dynamics of the actin-like protein Mbl of *Bacillus subtilis*. *Dev. Cell* **4**:19–28.
  21. Cervin, M. A., G. B. Spiegelman, B. Raether, K. Ohlsen, M. Perego, and J. A. Hoch. 1998. A negative regulator linking chromosome segregation to developmental transcription in *Bacillus subtilis*. *Mol. Microbiol.* **29**:85–95.
  22. Chang, L., and R. D. Goldman. 2004. Intermediate filaments mediate cytoskeletal crosstalk. *Nat. Rev. Mol. Cell Biol.* **5**:601–613.
  23. Cook, W. R., T. J. MacAlister, and L. I. Rothfield. 1986. Compartmentalization of the periplasmic space at division sites in gram-negative bacteria. *J. Bacteriol.* **168**:1430–1438.
  24. Cordell, S. C., and J. Löwe. 2001. Crystal structure of the bacterial cell division regulator MinD. *FEBS Lett.* **492**:160–165.
  25. Coulombe, P. A., and P. Wong. 2004. Cytoplasmic intermediate filaments revealed as dynamic and multipurpose scaffolds. *Nat. Cell Biol.* **6**:699–706.
  26. Dai, K., and J. Lutkenhaus. 1992. The proper ratio of FtsZ to FtsA is required for cell division to occur in *Escherichia coli*. *J. Bacteriol.* **174**:6145–6151.
  27. Daniel, R. A., and J. Errington. 2003. Control of cell morphogenesis in bacteria: two distinct ways to make a rod-shaped cell. *Cell* **113**:767–776.
  28. de Boer, P., R. E. Crossley, and L. I. Rothfield. 1992. Roles of MinC and MinD in the site-specific septation block mediated by the MinCDE system of *Escherichia coli*. *J. Bacteriol.* **174**:63–70.
  29. Defeu-Soufo, H. J., and P. L. Graumann. 2005. *Bacillus subtilis* actin-like protein MreB influences the positioning of the replication machinery and requires membrane proteins MreC/D and other actin-like proteins for proper localization. *BMC Cell Biol.* **6**:10.
  30. Den Blaauwen, T., M. E. Aarsman, N. O. Vischer, and N. Nanninga. 2003. Penicillin-binding protein PBP2 of *Escherichia coli* localizes preferentially in the lateral wall and at mid-cell in comparison with the old cell pole. *Mol. Microbiol.* **47**:539–547.
  31. de Pedro, M., C. Grunfelder, and H. Schwarz. 2004. Restricted mobility of surface proteins in the polar regions of *Escherichia coli*. *J. Bacteriol.* **186**:2594–2602.
  32. de Pedro, M., H. Schwarz, and A. L. Koch. 2003. Patchiness of murein insertion into the sidewall of *Escherichia coli*. *Microbiology* **149**:1753–1761.
  33. de Pedro, M. A., J. C. Quintela, J. V. Holtje, and H. Schwarz. 1997. Murein segregation in *Escherichia coli*. *J. Bacteriol.* **179**:2823–2834.
  34. de Pedro, M. A., K. D. Young, J.-V. Holtje, and H. Schwarz. 2003. Branching of *Escherichia coli* cells arises from multiple sites of inert peptidoglycan. *J. Bacteriol.* **185**:1147–1152.
  35. Divakaruni, A. V., R. R. Loo, Y. Xie, J. A. Loo, and J. W. Gober. 2005. The cell-shape protein MreC interacts with extracytoplasmic proteins including cell wall assembly complexes in *Caulobacter crescentus*. *Proc. Natl. Acad. Sci. USA* **102**:18602–18607.
  36. Drew, D., M. Osborn, and L. Rothfield. 2005. A polymerization-depolymerization model that accurately generates the self-sustained oscillatory system involved in bacterial division site placement. *Proc. Natl. Acad. Sci. USA* **102**:6114–6118.
  37. Dworkin, J., and R. Losick. 2002. Does RNA polymerase help drive chromosome segregation in bacteria? *Proc. Natl. Acad. Sci. USA* **99**:14089–14094.
  38. Dye, N. A., Z. Pincus, J. A. Theriot, L. Shapiro, and Z. Gitai. 2005. Two independent spiral structures control cell shape in *Caulobacter*. *Proc. Natl. Acad. Sci. USA* **102**:18608–18613.
  39. Ebersbach, G., and K. Gerdes. 2004. Bacterial mitosis: partitioning protein ParA oscillates in spiral-shaped structures and positions plasmids at mid-cell. *Mol. Microbiol.* **52**:385–398.
  40. Ebersbach, G., and K. Gerdes. 2001. The double par locus of virulence factor pB171: DNA segregation is correlated with oscillation of ParA. *Proc. Natl. Acad. Sci. USA* **98**:15078–15083.
  41. Ebersbach, G., and K. Gerdes. 2005. Plasmid segregation mechanisms. *Annu. Rev. Genet.* **39**:453–479.
  42. Edwards, D. H., and J. Errington. 1997. The *Bacillus subtilis* DivIVA protein targets to the division septum and controls the site-specificity of cell division. *Mol. Microbiol.* **24**:905–915.
  43. Edwards, D. H., H. B. Thomaidis, and J. Errington. 2000. Promiscuous targeting of *Bacillus subtilis* cell division protein DivIVA to division sites in *Escherichia coli* and fission yeast. *EMBO J.* **19**:2719–2727.
  44. Elowitz, M. B., M. G. Surette, P. E. Wolf, J. B. Stock, and S. Leibler. 1999. Protein mobility in the cytoplasm of *Escherichia coli*. *J. Bacteriol.* **181**:197–203.
  45. Erickson, H., D. Taylor, K. Taylor, and D. Bramhill. 1996. Bacterial cell division protein FtsZ assembles into protofilament sheets and minirings, structural homologs of tubulin polymers. *Proc. Natl. Acad. Sci. USA* **93**:519–523.
  46. Erickson, H. P. 2001. The FtsZ protofilament and attachment of ZipA—structural constraints on the FtsZ power stroke. *Curr. Opin. Cell Biol.* **13**:55–60.
  47. Errington, J., R. A. Daniel, and D. J. Scheffers. 2003. Cytokinesis in bacteria. *Microbiol. Mol. Biol. Rev.* **67**:52–65.
  48. Espeli, O., C. Lee, and K. J. Mariani. 2003. A physical and functional interaction between *Escherichia coli* FtsK and topoisomerase IV. *J. Biol. Chem.* **278**:44639–44644.
  49. Espeli, O., P. Nurse, C. Levine, C. Lee, and K. J. Mariani. 2003. SetB: an integral membrane protein that affects chromosome segregation in *Escherichia coli*. *Mol. Microbiol.* **50**:495–509.
  50. Esue, E., D. Wirtz, and Y. Tseng. 2006. GTPase activity, structure, and mechanical properties of filaments assembled from bacterial cytoskeleton protein MreB. *J. Bacteriol.* **188**:968–976.
  51. Esue, O., M. Cordero, D. Wirtz, and Y. Tseng. 2005. The assembly of MreB, a prokaryotic homolog of actin. *J. Biol. Chem.* **280**:2628–2635.
  52. Esue, O., Y. Tseng, and D. Wirtz. 2005. The rapid onset of elasticity during the assembly of the bacterial cell-division protein FtsZ. *Biochem. Biophys. Res. Commun.* **333**:508–516.
  53. Figge, R. M., A. V. Divakaruni, and J. W. Gober. 2004. MreB, the cell shape-determining bacterial actin homologue, co-ordinates cell wall morphogenesis in *Caulobacter crescentus*. *Mol. Microbiol.* **51**:1321–1332.
  54. Formstone, A., and J. Errington. 2005. A magnesium-dependent *mreB* null mutant: implications for the role of *mreB* in *Bacillus subtilis*. *Mol. Microbiol.* **55**:1646–1657.
  55. Garner, E. C., C. S. Campbell, and R. D. Mullins. 2004. Dynamic instability in a DNA-segregating prokaryotic actin homolog. *Science* **306**:1021–1025.
  56. Gelles, J., and R. Landick. 1998. RNA polymerase as a molecular motor. *Cell* **93**:13–16.
  57. Ghosh, A. S., and K. D. Young. 2005. Helical disposition of proteins and lipopolysaccharide in the outer membrane of *Escherichia coli*. *J. Bacteriol.* **187**:1913–1922.
  58. Gibbs, K. A., D. D. Isaac, J. Xu, R. W. Hendrix, T. J. Silhavy, and J. A. Theriot. 2004. Complex spatial distribution and dynamics of an abundant *Escherichia coli* outer membrane protein, LamB. *Mol. Microbiol.* **53**:1771–1783.
  59. Gitai, Z. 2005. The new bacterial cell biology: moving parts and subcellular architecture. *Cell* **120**:577–586.
  60. Gitai, Z., N. Dye, and L. Shapiro. 2004. An actin-like gene can determine cell polarity in bacteria. *Proc. Natl. Acad. Sci. USA* **101**:8643–8648.
  61. Gitai, Z., N. A. Dye, A. Reisenauer, M. Wachi, and L. Shapiro. 2005. MreB actin-mediated segregation of a specific region of a bacterial chromosome. *Cell* **120**:329–341.
  62. Godfrin-Estevenson, A. M., F. Pasta, and D. Lane. 2002. The *parAB* gene products of *Pseudomonas putida* exhibit partition activity in both *P. putida* and *Escherichia coli*. *Mol. Microbiol.* **43**:39–49.

63. Goehring, N., and J. Beckwith. 2005. Diverse paths to midcell: assembly of the bacterial cell division machinery. *Curr. Biol.* **15**:R514–R526.
64. Gueiros-Filho, F. J., and R. Losick. 2002. A widely conserved bacterial cell division protein that promotes assembly of the tubulin-like protein FtsZ. *Genes Dev.* **16**:2544–2556.
65. Haeusser, D. P., R. L. Schwartz, A. M. Smith, M. E. Oates, and P. A. Levin. 2004. EzrA prevents aberrant cell division by modulating assembly of the cytoskeletal protein FtsZ. *Mol. Microbiol.* **52**:801–814.
66. Hale, C., and P. de Boer. 1997. Direct binding of FtsZ to ZipA, an essential component of the septal ring structure that mediates cell division in *E. coli*. *Cell* **88**:175–185.
67. Hale, C. A., A. C. Rhee, and P. A. de Boer. 2000. ZipA-induced bundling of FtsZ polymers mediated by an interaction between C-terminal domains. *J. Bacteriol.* **182**:5153–5166.
68. Hayashi, I., T. Oyama, and K. Morikawa. 2001. Structural and functional studies of MinD ATPase: implications for the molecular recognition of the bacterial cell division apparatus. *EMBO J.* **20**:1819–1828.
69. Hayes, F., and D. Barilla. 2006. The bacterial segrosome: a dynamic nucleoprotein machine for DNA trafficking and segregation. *Nat. Rev. Microbiol.* **4**:133–143.
70. Hegemann, J., R. Herrmann, and F. Mayer. 2002. Cytoskeletal elements in the bacterium *Mycoplasma pneumoniae*. *Naturwissenschaften* **89**:453–458.
71. Helfand, B. T., L. Chang, and R. D. Goldman. 2004. Intermediate filaments are dynamic and motile elements of cellular architecture. *J. Cell Sci.* **117**:133–141.
72. Herrmann, H., and U. Aebi. 2004. Intermediate filaments: molecular structure, assembly mechanism, and integration into functionally distinct intracellular scaffolds. *Annu. Rev. Biochem.* **73**:749–789.
73. Higashitani, A., Y. Ishii, Y. Kato, and K. Koriuchi. 1997. Functional dissection of a cell-division inhibitor, SulA, of *Escherichia coli* and its negative regulation by Lon. *Mol. Gen. Genet.* **254**:351–357.
74. Hiraga, S., T. Ogura, H. Niki, C. Ichinose, and H. Mori. 1990. Positioning of replicated chromosomes in *Escherichia coli*. *J. Bacteriol.* **172**:31–39.
75. Hu, S., A. Mukherjee, S. Pichoff, and J. Lutkenhaus. 1999. The MinC component of the division site selection system in *Escherichia coli* interacts with FtsZ to prevent polymerization. *Proc. Natl. Acad. Sci. USA* **96**:14819–14824.
76. Hu, Z., E. Gogol, and J. Lutkenhaus. 2002. Dynamic assembly of MinD on phospholipid vesicles regulated by ATP and MinE. *Proc. Natl. Acad. Sci. USA* **99**:6761–6766.
77. Hu, Z., and J. Lutkenhaus. 2003. A conserved sequence at the C-terminus of MinD is required for binding to the membrane and targeting MinC to the septum. *Mol. Microbiol.* **47**:345–355.
78. Hu, Z., and J. Lutkenhaus. 1999. Topological regulation in *Escherichia coli* involves rapid pole-to-pole oscillation of the division inhibitor MinC under the control of MinD and MinE. *Mol. Microbiol.* **34**:82–90.
79. Hu, Z., and J. Lutkenhaus. 2001. Topological regulation of cell division in *E. coli*: spatiotemporal oscillation of MinD occurs through stimulation of its ATPase activity by MinE and phospholipid. *Mol. Cell* **7**:1337–1343.
80. Huang, J., C. Cao, and J. Lutkenhaus. 1996. Interaction between FtsZ and inhibitors of cell division. *J. Bacteriol.* **178**:5080–5085.
81. Huang, K. C., Y. Meir, and N. S. Wingreen. 2003. Dynamic structures in *Escherichia coli*: spontaneous formation of MinE rings and MinD polar zones. *Proc. Natl. Acad. Sci. USA* **100**:12724–12728.
82. Huecas, S., and J. M. Andreu. 2003. Energetics of the cooperative assembly of cell division protein FtsZ and the nucleotide hydrolysis switch. *J. Biol. Chem.* **278**:46146–46154.
83. Huitema, E., S. Pritchard, D. Matteson, S. K. Radhakrishnan, and P. H. Viollier. 2006. Bacterial birth scar proteins mark future flagellum assembly site. *Cell* **124**:1025–1037.
84. Hunding, A., G. Ebersbach, and K. Gerdes. 2003. A mechanism for ParB-dependent waves of ParA, a protein related to DNA segregation during cell division in prokaryotes. *J. Mol. Biol.* **329**:35–43.
85. Hurley, J., and B. Wendland. 2002. Endocytosis: driving membranes around the bend. *Cell* **111**:143–146.
86. Ireton, K., N. W. Gunther IV, and A. D. Grossman. 1994. *spoII* is required for normal chromosome segregation as well as the initiation of sporulation in *Bacillus subtilis*. *J. Bacteriol.* **176**:5320–5329.
87. Ishino, F., W. Park, S. Tomioka, S. Tamaki, I. Takase, K. Kunugita, H. Matsuzawa, S. Asoh, T. Ohta, B. G. Spratt, and M. Matsuhashi. 1986. Peptidoglycan synthetic activities in membranes of *Escherichia coli* caused by overproduction of penicillin-binding protein 2 and RodA protein. *J. Biol. Chem.* **261**:7024–7031.
88. Iwai, N., T. Ebata, H. Nagura, T. Kitasume, K. Nagai, and M. Wachi. 2004. Structure-activity relationship of S-benzylisothiourea derivatives to induce spherical cells in *Escherichia coli*. *Biosci. Biotechnol. Biochem.* **68**:2265–2269.
89. Izard, J., W. A. Samsonoff, M. B. Kinoshita, and R. J. Limberger. 1999. Genetic and structural analyses of cytoplasmic filaments of wild-type *Treponema phagedenis* and a flagellar filament-deficient mutant. *J. Bacteriol.* **181**:6739–6746.
90. Janakiraman, A., and M. B. Goldberg. 2004. Evidence for polar positional information independent of cell division and nucleoid occlusion. *Proc. Natl. Acad. Sci. USA* **101**:835–840.
91. Jenkins, C., R. Samudrala, I. Anderson, B. P. Hedlund, G. Petroni, N. Michailova, N. Pinel, R. Overbeek, G. Rosati, and J. T. Staley. 2002. Genes for the cytoskeletal protein tubulin in the bacterial genus *Prostheco bacter*. *Proc. Natl. Acad. Sci. USA* **99**:17049–17054.
92. Jensen, R. B., and K. Gerdes. 1999. Mechanism of DNA segregation in prokaryotes: ParM partitioning protein of plasmid R1 co-localizes with its replicon during the cell cycle. *EMBO J.* **18**:4076–4084.
93. Jensen, R. B., and K. Gerdes. 1997. Partitioning of plasmid R1. The ParM protein exhibits ATPase activity and interacts with the centromere-like ParR-parC complex. *J. Mol. Biol.* **269**:505–513.
94. Jensen, R. B., R. Lurz, and K. Gerdes. 1998. Mechanism of DNA segregation in prokaryotes: replicon pairing by parC of plasmid R1. *Proc. Natl. Acad. Sci. USA* **95**:8550–8555.
95. Jones, L., R. Carballido-Lopez, and J. Errington. 2001. Control of cell shape in bacteria: helical actin-like filaments in *Bacillus subtilis*. *Cell* **104**:913–922.
96. Justice, S. S., J. Garcia-Lara, and L. Rothfield. 2000. Cell division inhibitors SulA and MinC/MinD block septum formation at different steps in the assembly of the *Escherichia coli* division machinery. *Mol. Microbiol.* **37**:410–423.
97. Kelly, A., M. Sackett, N. Din, E. Quardokus, and Y. Brun. 1998. Cell cycle-dependent transcriptional and proteolytic regulation of FtsZ in *Caulobacter*. *Genes Dev.* **12**:880–893.
98. Kerr, R. A., H. Levine, T. J. Sejnowski, and W. J. Rappel. 2006. Division accuracy in a stochastic model of Min oscillations in *Escherichia coli*. *Proc. Natl. Acad. Sci. USA* **103**:347–352.
99. Kim, H. J., M. J. Calcutt, F. J. Schmidt, and K. F. Chater. 2000. Partitioning of the linear chromosome during sporulation of *Streptomyces coelicolor* A3(2) involves an *oriC*-linked *parAB* locus. *J. Bacteriol.* **182**:1313–1320.
100. King, G. F., Y.-L. Shih, M. W. Maciejewski, N. P. S. Bains, B. Pan, S. Rowland, G. P. Mullen, and L. I. Rothfield. 2000. Structural basis for the topological specificity function of MinE. *Nat. Struct. Biol.* **7**:1013–1017.
101. Komeili, A., Z. Li, D. K. Newman, and G. J. Jensen. 2005. Magnetosomes are cell membrane invaginations organized by the actin-like protein MamK. *Science* **311**:242–245.
102. Koonin, E. 1993. A superfamily of ATPases with diverse functions containing either classical or deviant ATP-binding motif. *J. Mol. Biol.* **229**:1165–1174.
103. Koradi, R., M. Billeter, and K. Wuthrich. 1996. MOLMOL: a program for display and analysis of macromolecular structures. *J. Mol. Graph.* **14**:51–55, 29–32.
104. Kreplak, L., U. Aebi, and H. Herrmann. 2004. Molecular mechanisms underlying the assembly of intermediate filaments. *Exp. Cell Res.* **301**:77–83.
105. Kruse, K. 2002. A dynamic model for determining the middle of *Escherichia coli*. *Biophys. J.* **82**:618–627.
106. Kruse, T., B. Blagoev, A. Lobner-Olesen, M. Wachi, K. Sasaki, N. Iwai, M. Mann, and K. Gerdes. 2006. Actin homolog MreB and RNA polymerase interact and are both required for chromosome segregation in *Escherichia coli*. *Genes Dev.* **20**:113–124.
107. Kruse, T., J. Bork-Jensen, and K. Gerdes. 2005. The morphogenetic MreBCD proteins of *Escherichia coli* form an essential membrane-bound complex. *Mol. Microbiol.* **55**:78–89.
108. Kruse, T., J. Møller-Jensen, A. Lobner-Olesen, and K. Gerdes. 2003. Dysfunctional MreB inhibits chromosome segregation in *Escherichia coli*. *EMBO J.* **22**:5283–5292.
109. Kürner, J., A. S. Frangakis, and W. Baumeister. 2005. Cryo-electron tomography reveals the cytoskeletal structure of *Spiroplasma melliferum*. *Science* **307**:436–438.
110. Lackner, L., D. Raskin, and P. de Boer. 2003. ATP-dependent interactions between *Escherichia coli* Min proteins and the phospholipid membrane in vitro. *J. Bacteriol.* **185**:735–749.
111. Lam, H., W. B. Schofield, and C. Jacobs-Wagner. 2006. A landmark protein essential for establishing and perpetuating the polarity of a bacterial cell. *Cell* **124**:1011–1023.
112. Lara, B., A. I. Rico, S. Petruzzelli, A. Santona, J. Dumas, J. Biton, M. Vicente, J. Mingorance, and O. Massidda. 2005. Cell division in cocci: localization and properties of the *Streptococcus pneumoniae* FtsA protein. *Mol. Microbiol.* **55**:699–711.
113. Leaver, M., and J. Errington. 2005. Roles for MreC and MreD proteins in helical growth of the cylindrical cell wall in *Bacillus subtilis*. *Mol. Microbiol.* **57**:1196–1209.
114. Lee, P. S., and A. D. Grossman. 2006. The chromosome partitioning proteins Soj (ParA) and Spo0J (ParB) contribute to accurate chromosome partitioning, separation of replicated sister origins, and regulation of replication initiation in *Bacillus subtilis*. *Mol. Microbiol.* **60**:853–869.
115. Lee, S., and C. W. Price. 1993. The *minCD* locus of *Bacillus subtilis* lacks the *minE* determinant that provides topological specificity to cell division. *Mol. Microbiol.* **7**:601–610.
116. Leonard, T. A., P. J. Butler, and J. Löwe. 2005. Bacterial chromosome

- segregation: structure and DNA binding of the Soj dimer—a conserved biological switch. *EMBO J.* **24**:270–282.
117. Levin, P., P. S. Margolis, P. Setlow, R. Losick, and D. Sun. 1992. Identification of *Bacillus subtilis* genes for septum placement and shape determination. *J. Bacteriol.* **174**:6717–6728.
  118. Levin, P. A., I. G. Kurtser, and A. D. Grossman. 1999. Identification and characterization of a negative regulator of FtsZ ring formation in *Bacillus subtilis*. *Proc. Natl. Acad. Sci. USA* **96**:9642–9647.
  119. Levin, P. A., and R. Losick. 1996. Transcription factor Spo0A switches the localisation of the cell division protein FtsZ from a medial to a bipolar pattern in *Bacillus subtilis*. *Genes Dev.* **10**:478–488.
  120. Lim, G. E., A. I. Derman, and J. Pogliano. 2005. Bacterial DNA segregation by dynamic SopA polymers. *Proc. Natl. Acad. Sci. USA* **102**:17658–17663.
  121. Lin, D. C., and A. D. Grossman. 1998. Identification and characterization of a bacterial chromosome partitioning site. *Cell* **92**:675–685.
  122. Löwe, J., and L. A. Amos. 1998. Crystal structure of the bacterial cell-division protein FtsZ. *Nature* **391**:203–206.
  123. Löwe, J., and L. A. Amos. 1999. Tubulin-like protofilaments in Ca<sup>2+</sup>-induced FtsZ sheets. *EMBO J.* **18**:2364–2371.
  124. Löwe, J., H. Li, K. H. Downing, and E. Nogales. 2001. Refined structure of alpha beta-tubulin at 3.5 Å resolution. *J. Mol. Biol.* **313**:1045–1057.
  125. Lu, C., J. Stricker, and H. P. Erickson. 1998. FtsZ from *Escherichia coli*, *Azotobacter vinelandii*, and *Thermotoga maritima*—quantitation, GTP hydrolysis, and assembly. *Cell Motil. Cytoskelet.* **40**:71–86.
  126. Lutkenhaus, J., and M. Sundaramoorthy. 2003. MinD and role of the deviant Walker A motif, dimerization and membrane binding in oscillation. *Mol. Microbiol.* **48**:295–303.
  127. Ma, L., G. F. King, and L. Rothfield. 2003. Mapping the MinE site involved in interaction with the MinD division site selection protein. *J. Bacteriol.* **185**:4948–4955.
  128. Ma, L., and L. Rothfield. 2004. Positioning of the MinE binding site on the MinD surface suggests a plausible mechanism for activation of the *Escherichia coli* MinD ATPase during division site selection. *Mol. Microbiol.* **54**:99–108.
  129. Ma, X., D. Ehrhardt, and W. Margolin. 1996. Colocalization of cell division proteins FtsZ and FtsA to cytoskeletal structures in living *Escherichia coli* cells by using green fluorescent protein. *Proc. Natl. Acad. Sci. USA* **93**:12998–13003.
  130. MacAlister, T. J., W. Cook, R. Weigand, and L. Rothfield. 1987. Membrane-murein attachment at the leading edge of the division septum: a second murein-membrane structure associated with morphogenesis of the gram-negative bacterial division septum. *J. Bacteriol.* **169**:3945–3951.
  131. MacAlister, T. J., B. MacDonald, and L. I. Rothfield. 1983. The periseptal annulus: an organelle associated with cell division in gram-negative bacteria. *Proc. Natl. Acad. Sci. USA* **80**:1372–1376.
  132. Maciver, S. K. 1998. How ADF/cofilin depolymerizes actin filaments. *Curr. Opin. Cell Biol.* **10**:140–144.
  133. Margolin, W. 2005. Bacterial mitosis: actin in a new role at the origin. *Curr. Biol.* **15**:R259–R261.
  134. Marston, A. L., and J. Errington. 1999. Dynamic movement of the ParA-like Soj protein of *B. subtilis* and its dual role in nucleoid organization and developmental regulation. *Mol. Cell* **4**:673–682.
  135. Marston, A. L., and J. Errington. 1999. Selection of the midcell division site in *Bacillus subtilis* through MinD-dependent polar localization and activation of MinC. *Mol. Microbiol.* **33**:84–96.
  136. Marston, A. L., H. B. Thomaidis, D. H. Edwards, M. E. Sharpe, and J. Errington. 1998. Polar localization of the MinD protein of *Bacillus subtilis* and its role in selection of the mid-cell division site. *Genes Dev.* **12**:3419–3430.
  137. McNally, F. J., and R. D. Vale. 1993. Identification of katanin, an ATPase that severs and disassembles stable microtubules. *Cell* **75**:419–429.
  138. Meinhardt, H., and P. de Boer. 2001. Pattern formation in *Escherichia coli*: a model for the pole-to-pole oscillations of min proteins and the localization of the division site. *Proc. Natl. Acad. Sci. USA* **98**:14202–14207.
  139. Meng, K., and R. Pfister. 1980. Intracellular structures of *Mycoplasma pneumoniae* revealed after membrane removal. *J. Bacteriol.* **144**:390–399.
  140. Michie, K. A., L. G. Monahan, P. L. Beech, and E. J. Harry. 2006. Trapping of a spiral-like intermediate of the bacterial cytokinetic protein FtsZ. *J. Bacteriol.* **188**:1680–1690.
  141. Mileykovskaya, E., and W. Dowhan. 2000. Visualization of phospholipid domains in *Escherichia coli* by using the cardiolipin-specific fluorescent dye 10-N-nonyl acridine orange. *J. Bacteriol.* **182**:1172–1175.
  142. Mingorance, J., S. Rueda, M. Gomez-Puertas, A. Valencia, and M. Vicente. 1991. *Escherichia coli* FtsZ polymers contain mostly GTP and have a high nucleotide turnover. *Mol. Microbiol.* **41**:83–91.
  143. Mingorance, J., M. Tados, M. Vicente, J. M. Gonzalez, G. Rivas, and M. Velez. 2005. Visualization of single *Escherichia coli* FtsZ filament dynamics with atomic force microscopy. *J. Biol. Chem.* **280**:20909–20914.
  144. Mohl, D. A., and J. W. Gober. 1997. Cell cycle-dependent polar localization of chromosome partitioning proteins in *Caulobacter crescentus*. *Cell* **88**:675–684.
  145. Möller-Jensen, J., J. Borch, M. Dam, R. B. Jensen, P. Roepstorff, and K. Gerdes. 2003. Bacterial mitosis: ParM of plasmid R1 moves plasmid DNA by an actin-like insertional polymerization mechanism. *Mol. Cell* **12**:1477–1487.
  146. Möller-Jensen, J., R. B. Jensen, L. Lachner, J. Löwe, and K. Gerdes. 2002. Prokaryotic DNA segregation by an actin-like filament. *EMBO J.* **21**:3119–3127.
  147. Moriya, S., E. Tsujikawa, A. Hassan, K. Asai, T. Kodama, and N. Ogasawara. 1998. A *Bacillus subtilis* gene encoding a protein homologous to eukaryotic SMC proteins is necessary for chromosome partition. *Mol. Microbiol.* **29**:179–187.
  148. Mukherjee, A., C. Cao, and J. Lutkenhaus. 1998. Inhibition of FtsZ polymerization by SulA, an inhibitor of septation in *Escherichia coli*. *Proc. Natl. Acad. Sci. USA* **95**:2885–2890.
  149. Mukherjee, A., and J. Lutkenhaus. 1998. Dynamic assembly of FtsZ regulated by GTP hydrolysis. *EMBO J.* **17**:462–469.
  150. Niggli, V. 2001. Structural properties of lipid-binding sites in cytoskeletal proteins. *Trends Biochem. Sci.* **26**:604–611.
  151. Nilsen, T., A. W. Yan, G. Gale, and M. B. Goldberg. 2005. Presence of multiple sites containing polar material in spherical *Escherichia coli* cells that lack MreB. *J. Bacteriol.* **187**:6187–6196.
  152. Nogales, E., K. Downing, L. Amos, and J. Löwe. 1998. Tubulin and FtsZ form a distinct family of GTPases. *Nat. Struct. Biol.* **5**:451–458.
  153. Reference deleted.
  154. Nordström, K., and S. J. Austin. 1989. Mechanisms that contribute to the stable segregation of plasmids. *Annu. Rev. Genet.* **23**:37–69.
  155. Okinaka, R., K. Cloud, O. Hampton, A. Hoffmaster, K. Hill, P. Keim, T. Koehler, G. Lamke, S. Kumano, D. Manter, Y. Martinez, D. Ricke, R. Svensson, and P. Jackson. 1999. Sequence, assembly and analysis of pXO1 and pXO2. *J. Appl. Microbiol.* **87**:261–262.
  156. Okinaka, R. T., K. Cloud, O. Hampton, A. R. Hoffmaster, K. K. Hill, P. Keim, T. M. Koehler, G. Lamke, S. Kumano, D. Mahillon, D. Manter, Y. Martinez, D. Ricke, R. Svensson, and P. J. Jackson. 1999. Sequence and organization of pXO1, the large *Bacillus anthracis* plasmid harboring the anthrax toxin genes. *J. Bacteriol.* **181**:6509–6515.
  157. Oliva, M. A., S. C. Cordell, and J. Löwe. 2004. Structural insights into FtsZ protofilament formation. *Nat. Struct. Mol. Biol.* **11**:1243–1250.
  158. Petroni, G., S. Spring, K. H. Schleifer, F. Verni, and G. Rosati. 2000. Defensive extrusive ectosymbionts of *Euplodium* (*Ciliophora*) that contain microtubule-like structures are bacteria related to *Verrucomicrobia*. *Proc. Natl. Acad. Sci. USA* **97**:1813–1817.
  159. Pichoff, S., and J. Lutkenhaus. 2005. Tethering the Z-ring to the membrane through a conserved membrane targeting sequence in FtsA. *Mol. Microbiol.* **55**:1722–1734.
  160. Pichoff, S., and J. Lutkenhaus. 2002. Unique and overlapping roles for ZipA and FtsA in septal ring assembly in *Escherichia coli*. *EMBO J.* **21**:685–693.
  161. Pinho, M., and J. Errington. 2005. Recruitment of penicillin-binding protein PB2 to the division site of *Staphylococcus aureus* is dependent on its transpeptidation substrates. *Mol. Microbiol.* **55**:799–807.
  162. Pla, J., M. Sánchez, P. Palacios, M. Vicente, and M. Aldea. 1991. Preferential cytoplasmic location of FtsZ, a protein essential for *Escherichia coli* septation. *Mol. Microbiol.* **5**:1681–1686.
  163. Poindexter, J., and J. Hagenzieker. 1982. Novel peptidoglycans in *Caulobacter* and *Asticcacaulis* spp. *J. Bacteriol.* **150**:332–347.
  164. Pollard, T. D., L. Blanchoin, and R. D. Mullins. 2000. Molecular mechanisms controlling actin filament dynamics in nonmuscle cells. *Annu. Rev. Biophys. Biomol. Struct.* **29**:545–576.
  165. Quardokus, E., N. Din, and Y. Brun. 1996. Cell cycle regulation and cell type-specific localization of the FtsZ division initiation protein in *Caulobacter*. *Proc. Natl. Acad. Sci. USA* **93**:6314–6319.
  166. Quisel, J. D., D. C. Lin, and A. D. Grossman. 1999. Control of development by altered localization of a transcription factor in *B. subtilis*. *Mol. Cell.* **4**:665–672.
  167. Raskin, D., and P. de Boer. 1999. MinDE-dependent pole-to-pole oscillation of division inhibitor MinC in *Escherichia coli*. *J. Bacteriol.* **181**:6419–6424.
  168. Raskin, D., and P. de Boer. 1999. Rapid pole-to-pole oscillation of a protein required for directing division to the middle of *Escherichia coli*. *Proc. Natl. Acad. Sci. USA* **96**:4971–4976.
  169. RayChaudhuri, D. 1999. ZipA is a MAP-Tau homolog and is essential for structural integrity of the cytokinetic FtsZ ring during bacterial cell division. *EMBO J.* **18**:2372–2383.
  170. Regula, J. T., G. Boguth, A. Gorg, J. Hegermann, F. Mayer, R. Frank, and R. Herrmann. 2001. Defining the mycoplasma 'cytoskeleton': the protein composition of the Triton X-100 insoluble fraction of the bacterium *Mycoplasma pneumoniae* determined by 2-D gel electrophoresis and mass spectrometry. *Microbiology* **147**:1045–1057.
  171. Roeben, A., C. Kofler, I. Nagy, S. Nickell, F. Ulrich Hartl, and A. Bracher. 2006. Crystal structure of an archaeal actin homolog. *J. Mol. Biol.* **358**:145–156.
  172. Romberg, L., and P. A. Levin. 2003. Assembly dynamics of the bacterial cell

- division protein FtsZ: poised at the edge of stability. *Annu. Rev. Microbiol.* **57**:125–154.
173. Rosati, G., P. Lenzi, and F. Verni. 1993. Epixenosomes, peculiar episymbionts of the protozoan ciliate *Euplotidium itoi*: do their cytoplasmic tubules consist of tubulin? *Micron* **24**:465–471.
  174. Rothfield, L. 2003. New insights into the developmental history of the bacterial cell division site. *J. Bacteriol.* **185**:1125–1127.
  175. Rothfield, L., A. Taghbalout, and Y.-L. Shih. 2005. Spatial control of bacterial division-site placement. *Nat. Rev. Microbiol.* **31**:959–968.
  176. Rothfield, L., S. Justice, and J. Garcia-Lara. 1999. Bacterial cell division. *Annu. Rev. Genet.* **33**:423–448.
  177. Rowland, S. L., X. Fu, M. A. Sayed, Y. Zhang, W. R. Cook, and L. I. Rothfield. 2000. Membrane redistribution of the *Escherichia coli* MinD protein induced by MinE. *J. Bacteriol.* **182**:613–619.
  178. Rueda, S., M. Vicente, and J. Mingorance. 2003. Concentration and assembly of the division ring proteins FtsZ, FtsA, and ZipA during the *Escherichia coli* cell cycle. *J. Bacteriol.* **185**:3344–3351.
  179. Sackett, M., A. Kelly, and Y. Brun. 1998. Ordered expression of *ftsQA* and *ftsZ* during the *Caulobacter crescentus* cell cycle. *Mol. Microbiol.* **28**:421–434.
  180. Sakai, N., M. Yao, H. Itoy, N. Watanabe, F. Yumoto, M. Tanojura, and I. Tanaka. 2001. The three-dimensional structure of septum site-determining protein MinD from *Pyrococcus horikoshii* OT3 in complex with Mg-ATP. *Structure* **9**:817–826.
  181. Sawitzke, J. A., and S. Austin. 2000. Suppression of chromosome segregation defects of *Escherichia coli* muk mutants by mutations in topoisomerase I. *Proc. Natl. Acad. Sci. USA* **97**:1671–1676.
  182. Scheffers, D. J., L. J. Jones, and J. Errington. 2004. Several distinct localization patterns for penicillin-binding proteins in *Bacillus subtilis*. *Mol. Microbiol.* **51**:749–764.
  183. Schlieper, D., M. A. Oliva, J. M. Andreu, and J. Löwe. 2005. Structure of bacterial tubulin BtubA/B: evidence for horizontal gene transfer. *Proc. Natl. Acad. Sci. USA* **102**:9170–9175.
  184. Schwarz, U., A. Asmus, and H. Frank. 1969. Autolytic enzymes and cell division of *Escherichia coli*. *J. Mol. Biol.* **41**:419–429.
  185. Shapiro, L., H. H. McAdams, and R. Losick. 2002. Generating and exploiting polarity in bacteria. *Science* **298**:1942–1946.
  186. Shih, Y.-L., X. Fu, G. F. King, T. Le, and L. I. Rothfield. 2002. Division site placement in *E. coli*: mutations that prevent formation of the MinE ring lead to loss of the normal midcell arrest of growth of polar MinD membrane domains. *EMBO J.* **21**:3347–3357.
  187. Shih, Y.-L., T. Le, and L. Rothfield. 2003. Division site selection in *Escherichia coli* involves dynamic redistribution of Min proteins within coiled structures that extend between the two cell poles. *Proc. Natl. Acad. Sci. USA* **100**:7865–7870.
  188. Shih, Y. L., I. Kawagishi, and L. Rothfield. 2005. The MreB and Min cytoskeletal-like systems play independent roles in prokaryotic polar differentiation. *Mol. Microbiol.* **58**:917–928.
  189. Reference deleted.
  190. Shiomi, D., M. Yoshimoto, M. Homma, and I. Kawagishi. 2006. Helical distribution of the bacterial chemoreceptor via colocalization with the Sec protein translocation machinery. *Mol. Microbiol.* **60**:894–906.
  191. Slovak, P. M., G. H. Wadhams, and J. P. Armitage. 2005. Localization of MreB in *Rhodospirillum rubrum* under conditions causing changes in cell shape and membrane structure. *J. Bacteriol.* **187**:54–64.
  192. Sontag, C. A., J. T. Staley, and H. P. Erickson. 2005. In vitro assembly and GTP hydrolysis by bacterial tubulins BtubA and BtubB. *J. Cell Biol.* **169**:233–238.
  193. Soufo, H. J., and P. L. Graumann. 2003. Actin-like proteins MreB and Mbl from *Bacillus subtilis* are required for bipolar positioning of replication origins. *Curr. Biol.* **13**:1916–1920.
  194. Soufo, H. J. D., and P. L. Graumann. 2004. Dynamic movement of actin-like proteins within bacterial cells. *EMBO Rep.* **5**:789–794.
  195. Staley, J. T., H. Bouzek, and C. Jenkins. 2005. Eukaryotic signature proteins of *Prostheco bacter* de jonei and Gemmata sp. Wa-1 as revealed by in silico analysis. *FEMS Microbiol. Lett.* **243**:9–14.
  196. Stoker, N. G., J. M. Pratt, and B. G. Spratt. 1983. Identification of the *rodA* gene product of *Escherichia coli*. *J. Bacteriol.* **155**:854–859.
  197. Stricker, J., P. Maddox, E. D. Salmon, and H. P. Erickson. 2002. Rapid assembly dynamics of the *Escherichia coli* FtsZ-ring demonstrated by fluorescence recovery after photobleaching. *Proc. Natl. Acad. Sci. USA* **99**:3171–3175.
  198. Suefui, K., R. Valluzzi, and D. Raychaudhuri. 2002. Dynamic assembly of MinD into filament bundles mediated by ATP, phospholipids, and MinE. *Proc. Natl. Acad. Sci. USA* **99**:16776–16781.
  199. Sun, Q., and W. Margolin. 1998. FtsZ dynamics during the division cycle of live *Escherichia coli* cells. *J. Bacteriol.* **180**:2050–2056.
  200. Sweitzer, S., and J. Hinshaw. 1998. Dynamin undergoes a GTP-dependent conformational change causing vesiculation. *Cell* **93**:1021–1029.
  201. Szeto, J., N. F. Eng, S. Acharya, M. D. Rigden, and J. A. Dillon. 2005. A conserved polar region in the cell division site determinant MinD is required for responding to MinE-induced oscillation but not for localization within coiled arrays. *Res. Microbiol.* **156**:17–29.
  202. Szeto, T., S. Rowland, L. Rothfield, and G. F. King. 2002. Membrane localization of MinD is mediated by a C-terminal motif that is conserved across eubacteria, archaea, and chloroplasts. *Proc. Natl. Acad. Sci. USA* **99**:15693–15698.
  203. Szeto, T. H., S. Rowland, C. Habrukowich, and G. F. King. 2003. The MinD membrane targeting sequence is a transplantable lipid-binding helix. *J. Biol. Chem.* **279**:40050–40056.
  204. Taghbalout, A., L. Ma, and L. Rothfield. 2006. Role of MinD-membrane association in Min protein interactions. *J. Bacteriol.* **188**:2993–3001.
  205. Thanedar, S., and W. Margolin. 2004. FtsZ exhibits rapid movement and oscillation waves in helix-like patterns in *Escherichia coli*. *Curr. Biol.* **14**:1167–1173.
  206. Tilney, L. G., J. Bryan, D. J. Bush, K. Fujiwara, M. S. Mooseker, D. B. Murphy, and D. H. Snyder. 1973. Microtubules: evidence for 13 protofilaments. *J. Cell Biol.* **59**:267–275.
  207. Tinsley, E., and S. A. Khan. 2006. A novel FtsZ-like protein is involved in replication of the anthrax toxin-encoding pXO1 plasmid in *Bacillus anthracis*. *J. Bacteriol.* **188**:2829–2835.
  208. Townsend, R., D. B. Archer, and K. A. Plaskitt. 1980. Purification and preliminary characterization of *Spiroplasma fibrilis*. *J. Bacteriol.* **142**:694–700.
  209. Trachtenberg, S. 1998. Mollicutes—wall-less bacteria with internal cytoskeletons. *J. Struct. Biol.* **124**:244–256.
  210. Trachtenberg, S., and R. Gilad. 2001. A bacterial linear motor: cellular and molecular organization of the contractile cytoskeleton of the helical bacterium *Spiroplasma melliferum* BC3. *Mol. Microbiol.* **41**:827–848.
  211. Trusca, D., and D. Bramhill. 2002. Fluorescent assay for polymerization of purified bacterial FtsZ cell-division protein. *Anal. Biochem.* **307**:322–329.
  212. Trusca, D., S. Scott, C. Thompson, and D. Bramhill. 1998. Bacterial SOS checkpoint protein SulA inhibits polymerization of purified FtsZ cell division protein. *J. Bacteriol.* **180**:3946–3953.
  213. van den Ent, F., L. Amos, and J. Löwe. 2001. Bacterial ancestry of actin and tubulin. *Curr. Opin. Microbiol.* **4**:634–638.
  214. Van den Ent, F., L. Amos, and J. Löwe. 2001. Prokaryotic origin of the actin cytoskeleton. *Nature* **413**:39–44.
  215. van den Ent, F., and J. Löwe. 2000. Crystal structure of the cell division protein FtsA from *Thermotoga maritima*. *EMBO J.* **19**:5300–5307.
  216. van den Ent, F., J. Moller-Jensen, L. A. Amos, K. Gerdes, and J. Löwe. 2002. F-actin-like filaments formed by plasmid segregation protein ParM. *EMBO J.* **21**:6935–6943.
  217. Varley, A. W., and G. C. Stewart. 1992. The *divIVB* region of the *Bacillus subtilis* chromosome encodes homologs of *Escherichia coli* septum placement (MinCD) and cell shape (MreBCD) determinants. *J. Bacteriol.* **174**:6729–6742.
  218. Vorobiev, S., B. Strokopytov, D. G. Drubin, C. Frieden, S. Ono, J. Condeelis, P. A. Rubenstein, and S. C. Almo. 2003. The structure of nonvertebrate actin: implications for the ATP hydrolytic mechanism. *Proc. Natl. Acad. Sci. USA* **100**:5760–5765.
  219. Wachi, M., M. Doi, Y. Okada, and M. Matsuhashi. 1989. New *mre* genes *mreC* and *mreD*, responsible for formation of the rod shape of *Escherichia coli* cell. *J. Bacteriol.* **171**:6511–6516.
  220. Wachi, M., M. Doi, S. Tamaki, W. Park, S. Nakajima-Iijima, and M. Matsuhashi. 1987. Mutant isolation and molecular cloning of *mre* genes, which determine cell shape, sensitivity to mecillinam, and amount of penicillin-binding proteins in *Escherichia coli*. *J. Bacteriol.* **169**:4935–4940.
  221. Walker, G. C. 1987. The SOS response of *Escherichia coli*, p. 1346–1357. In F. C. Neidhardt, J. L. Ingraham, K. B. Low, B. Magasanik, M. Schaechter, and H. E. Umbarger (ed.), *Escherichia coli* and *Salmonella typhimurium*: cellular and molecular biology. American Society for Microbiology, Washington, D.C.
  222. Walker, J. E., M. Saraste, M. J. Runswick, and N. J. Gay. 1982. Distantly related sequences in the  $\alpha$ - and  $\beta$ -subunits of ATP synthase, myosin, kinases and other ATP-requiring enzymes and a common nucleotide binding fold. *EMBO J.* **1**:945–951.
  223. Wu, L. J., and J. Errington. 2003. RacA and the Spo-Spo0J system combine to effect polar chromosome segregation in sporulating *Bacillus subtilis*. *Mol. Microbiol.* **49**:1463–1475.
  224. Yamaichi, Y., and H. Niki. 2000. Active segregation by the *Bacillus subtilis* partitioning system in *Escherichia coli*. *Proc. Natl. Acad. Sci. USA* **97**:14656–14661.
  225. Yang, R., S. Bartle, R. Otto, A. Stassinopoulos, M. Rogers, L. Plamann, and P. Hartzell. 2004. AglZ is a filament-forming coiled-coil protein required for adventurous gliding motility of *Myxococcus xanthus*. *J. Bacteriol.* **186**:6168–6178.
  226. Zhou, H., and J. Lutkenhaus. 2003. Membrane binding by MinD involves insertion of hydrophobic residues within the C-terminal amphipathic helix into the bilayer. *J. Bacteriol.* **185**:4326–4335.